國 立 交 通 大 學

電信工程學系碩士班
碩士論文

序列之轉換域產生法及其在多輸入多輸出正交分頻多工系統之應用

Transform Domain Approach for Sequence Design and Its Applications to MIMO-OFDM Systems

研 究 生：蔡隆盛　　Student: Lung-Sheng Tsai

指導教授：蘇育德 博士　　Advisor: Dr. Yu Ted Su

中 華 民 國 九 十 三 年 六 月

序列之轉換域產生法及其在多輸入多輸出正交分頻多工系統之應用

Transform Domain Approach for Sequence Design and Its Applications to MIMO-OFDM Systems

研 究 生：蔡隆盛　　Student: Lung-Sheng Tsai

指導教授：蘇育德 博士　　Advisor: Dr. Yu T. Su

國立交通大學

電信工程學系碩士班

碩士論文

A Thesis
Submitted to Institute of Communication Engineering
College of Electrical Engineering and Computer Science
National Chiao Tung University
in Partial Fulfillment of the Requirements
for the Degree of
Master of Science
in
Communication Engineering
June 2004
Hsinchu, Taiwan, Republic of China

中 華 民 國 九 十 三 年 六 月

序列之轉換域產生法及其在多輸入多輸出正交分頻多工系統之應用

研究生：蔡隆盛　　指導教授：蘇育德博士

國立交通大學電信工程學系碩士班

中文摘要

多輸入多輸出系統(MIMO)搭配正交分頻多工(OFDM)技術具有相當大的潛力可以達到更高的傳輸容量，在實際系統方面已有相當多的研究成果，但仍有一些關鍵性的議題待克服。本論文重點在於 MIMO-OFDM 系統所需的前置訊號設計。

在本論文中，我們提出一系統化的轉換域序列產生法；此方法可以產生一組具有良好自相關(autocorrelation)與互相關(cross-correlation)性質的序列。這些序列也可由有限訊號群集點(finite constellation points)經由反向離散傅利葉轉換來產生。一些已有的序列可以用我們所提出的方式產生，然而我們提出的序列較舊有者受較少的限制。基於我們所提出的概念，這些建立一維序列的方法可以輕易地延伸到多維陣列序列(multi-dimensional array sequences)的建構。

利用本文所介紹的新序列，我們提出了可用於 MIMO-OFDM 系統的前置信號結構；我們也討論了基於此結構對應的頻率漂移估測以及通道估測演算法。由電腦模擬的結果可知我們所提出的作法的確達到了最佳的效能表現。

Transform Domain Approach for Sequence Design and Its Applications to MIMO-OFDM Systems

Student : Lung-Sheng Tsai Advisor : Yu T. Su

Department of Communication Engineering

National Chiao Tung University

Abstract

Multiple antenna based Multiple-Input Multiple-Output (MIMO) systems employing Orthogonal Frequency Division Multiplexing (OFDM) have the potential of achieving the capacity promised by information theoretical prediction. Though much progress toward a practical high rate MIMO-OFDM system has been made, many related system design issues remain to be settled. This thesis sets forth to solve the critical issue of the preamble design for MIMO-OFDM systems.

We present a systematic method based on the frequency (transform) domain characterization to generate a new family of sequences with the desired autocorrelation and cross-correlation properties. Sequences having the desired properties can then be generated by taking inverse transform of some finite constellation points (BPSK, QPSK, ... etc.). We also demonstrate that some existing sequences can easily be generated by our approach but our new family of sequences renders less constraints. The proposed approach can easily be extended to synthesize two dimensional arrays or even higher dimensions waveforms that possess the desired multi-dimensional correlation properties.

A preamble structure based on our new sequence family is suggested and algorithms for frequency offset and channel estimations in MIMO-OFDM systems are developed. Both theoretical analysis and computer simulation show that these algorithms yield optimal performance.

Contents

English Abstract **i**

Contents **ii**

List of Figures **iv**

1 Introduction **1**

2 Orthogonal Sequences and Related Properties **4**

2.1 Welch bound (Sarwate bound) 5

2.2 A new set of orthogonal sequences 7

2.2.1 Notation and definitions 7

2.2.2 FZC sequences 8

2.2.3 Generation of the new set of sequences 8

2.2.4 Properties of the new set of sequences 9

2.2.5 Summary of the new set of sequences 12

2.3 PS Sequences 12

2.3.1 Generation of the PS sequence 13

2.3.2 Properties of the PS sequences 14

2.4 Comparison 14

3 The Basis Sequence of the PS Sequences **19**

3.1 Preliminary 19

3.2 Generating basis sequences 20

4 Multi-dimensional Arrays **29**

4.1 Array correlation functions 29

4.2 New 2D arrays 30

4.3 Properties of the new proposed 2D arrays 31

4.4 Extension to multi-dimensional arrays 32

5 Preamble Structure for MIMO-OFDM WLAN Systems **34**

5.1 Backgrounds 34

5.1.1 MIMO-OFDM WLAN systems 34

5.2 Proposed preamble structure 34

5.2.1 Cyclic prefix 36

5.2.2 Length of the training sequence 36

5.2.3 Constraints on the constellation of training symbols 37

5.3 Simulation environment 38

6 Fine Frequency Offset Estimation and Channel Estimation **40**

6.1 Timing and frequency synchronization for SISO OFDM systems 40

6.1.1 Schmidl and Cox's algorithms 41

6.2 Frequency synchronization schemes for MIMO-OFDM systems 43

6.3 Channel Estimation 44

6.3.1 System model 44

6.3.2 A least square error channel estimator 46

6.3.3 Numerical results 47

7 Conclusion **51**

Bibliography **52**

List of Figures

2.1 Construct the $C_i(\lambda)$'s from the DFT points of the basis sequence. 16

2.2 $\Theta_{c_i,c_i}(\lambda)$'s for $0 < i < K$ are simply frequency-shifting functions of $\Theta_{c_0,c_0}(\lambda)$. 17

2.3 The autocorrelation function of the new sequence.($K = 2, N_c = 32$, and $N = KN_c = 64$) 17

2.4 The autocorrelation function of the PS sequence.($K = 4, N_b^2 = 16$, and $N_s = KN_b^2 = 64$) 18

3.1 3-IDFT of $\vec{b}_i$. The elements of the matrix G, $g_0 \sim g_8$, are complex number with unit magnitude. 20

3.2 Rate-expanding and time-shifting. The time-domain sequences and their corresponding frequency-domain sequences are showed. 22

3.3 Generate the new sequence with perfect periodic AC property. All frequency components are of equal magnitude. 23

3.4 $g.c.d.(m,\ N_b) = 1$. Magnitude plot for the DFT of each column vector of $G^{(m)}$. 27

3.5 $g.c.d.(m,\ N_b) = 1$. AC function of the sequence of $m = 3$. 27

3.6 $g.c.d.(m,\ N_b) \neq 1$. Magnitude plot for the DFT of each column vector of $G^{(m)}$. 28

3.7 $g.c.d.(m,\ N_b) \neq 1$. AC function of the sequence of $m = 2$. 28

4.1 (a) Construct the $F^{(0)}(U,V)$ from the two-dimensional DFT points of the basis array. (b) Different symbols represent the non-zero positions of $F^{(i)}(U,V)$ for different i's; ($K_1 = 2$, $K_2 = 2$, $N_1 = 4$, and $N_2 = 5$.) 31
4.2 Magnitude plot for the two-dimensional periodic AC function of proposed array sequences, $|R_{C^{(i)}}|$. ($K_1 = 2$, $K_2 = 2$, $N_1 = 4$, and $N_2 = 5$.) 32

5.1 OFDM training structure in IEEE 802.11a standard. (We will redesign the long training sequences.) 35
5.2 A time orthogonal preamble for a MIMO configuration with 2 transmit antennas. (The guard intervals are not shown in this figure.) 36
5.3 A coded orthogonal preamble for a MIMO configuration with 2 transmit antennas. 36
5.4 Suggested long training symbol structure for a MIMO configuration with 2 transmit antennas. 37
5.5 Transmitter block diagram for the OFDM PHY. 37

6.1 A typical result of Schmidl and Cox's synchronization algorithm. The estimated frequency offset is in unit of the subcarrier spacing. (Parameters: r.m.s. delay spread = 50ns, frequency offset = 0.3 subcarrier spacing, and SNR = 10dB.) 42
6.2 MSE of the frequency offset estimator in different multi-path environments (2Txs and 1 Rx). Frequency offset = 0.3 subcarrier spacing. 43
6.3 MSE of the frequency offset estimator for systems of different number of transmit antennas. (Frequency offset=0.3 subcarrier spacing and r.m.s. delay spread=50ns.) 44
6.4 A system with two transmit antennas and one receive antenna. 45
6.5 Mean squared channel estimation error. Noise variance can be reduced by averaging. 49

6.6 Mean squared channel estimation error for different channel delay spread.(Guard Interval = 16 samples.) 50

Chapter 1

Introduction

It has been shown that the capacity of a wireless communication system can be greatly increased by employing multiple transmit and receive antennas. The Orthogonal Frequency Division Multiplexing (OFDM) scheme, because of its proven superiority over other wideband transmission alternatives, is a natural candidate choice for use in conjunction with the Multiple-Input Multiple-Output (MIMO) technique. Although the data rate of a MIMO-OFDM system can be increased drastically, the number of system parameters that need to be estimated in either the initial link set-up stage or the regular transmission stage increases as well.

Efforts to extend some existing OFDM based standards or products like the Local Area Network (WLAN) (IEEE 802.11a) and Direct Video Broadcasting (DVB) such that they are compatible with a MIMO scenario have been actively pursued recently. The main purpose of this thesis is to design a preamble structure that is optimal for MIMO-OFDM based WLAN systems. The main utility of a preamble is to facilitate the receiver's synchronization and channel estimation tasks (data-aided synchronization and channel estimation) with as little overhead as possible. An ideal preamble waveform should therefore has high time and frequency resolutions while render little or no ambiguity, be it resulted from multiple propagation paths or interference bearing similar structures. These desired properties usually entail a preamble that has a Dirac-like auto-correlation (AC) and, if a family of preambles is in question, zero cross-correlation

(CC). Practical considerations also require that the length of the preamble be arbitrary and the family size be as large as possible while maintaining the above two properties. Unfortunately, as far as a family of preamble sequences is concerned, one can not have all the nice properties simultaneously. The trade-offs are discussed in Chapter 2.

It is instructive to consider a multiple-transmit-antenna signal as sum of different user signals in a multiple access systems. Our investigation begins with the consideration of some signature sequences that are being used in CDMA systems. Gold code [1] is a popular choice but it is not appropriate for use as a training sequence of an OFDM system for the following two reasons. Firstly, the length of the Gold code is limited to 2^m-1 while an OFDM frame size is often a power of 2 because of FFT implementation. Secondly, the mutual interference caused by cross-correlation is not as low as desired especially when short period code is used. Scholtz and Welch presented a class of sequences based on [2] *Group Characters*. These sequences have similar autocorrelation properties as m-sequences, and their cross-correlations can be smaller than those of Gold codes. But the sequence duration must be a prime number and the cross-correlation is still not low enough when the sequence duration is short. Walsh-Hadamard sequences are orthogonal (zero cross-correlation) in a frame-synchronous condition but do not possess the desired Dirac-like autocorrelation property, suffering from severe self-interference when multiple propagation paths exist.

As one cannot have both the ideal auto-correlation and cross-correlation, an alternate design philosophy is to sacrifice some of the desired properties that do not bring in either self interference or interference from other system users. For example, the autocorrelation at time-lags larger than the transmission channel's multipath delay do not contribute to self-interference (inter-symbol interference, ISI). A set of sequences, called the *PS sequences* does have some desirable properties that can be applied to be the preamble design for the case of interest to us. In the ensuing chapter we present a new family of preamble sequences that have the desired AC and CC properties similar to

those of the PS sequences but have less constraint on the sequence durations. We propose a transform (frequency) domain approach such that the AC and CC requirements are directly transformed into the frequency domain identities. Although this approach has been suggested to generate complex sequences with Dirac-like aperiodic AC property and study some combinatorial design problems, as far as we know, it has never applied to the design of preamble sequences with predetermined periodic AC and CC functions.

Our approach also has the benefit of interpreting the PS sequences from the frequency (transform) domain's viewpoint. The sequences proposed in [8] have perfect AC properties and were used to generate the PS sequences. In Chapter 3, we explain why the sequences of [8] can have perfect AC properties by using similar concepts of chapter 2. In Chapter 4, We extend the concepts developed for one-dimensional sequences to multi-dimensional array sequences. In Chapter 5, we propose a preamble structure for MIMO-OFDM WLAN systems, and show why our new sequence has some flexibility when applied in OFDM systems. Chapter 6 presents algorithms for frequency offset estimation and channel estimation. We show that the proposed preamble structure can achieve the lower bound of the channel estimation mean square error.

Chapter 2

Orthogonal Sequences and Related Properties

Park *et al.* [3] invented a set of sequences (called *PS sequences*) that has excellent periodic autocorrelation and cross-correlation properties. The periodic AC of the sequence is 0 except at periodic intervals and the CC function between properly selected sequences is identical to 0 everywhere. Because of the AC and CC properties, they propose to use the PS sequences as the signature sequences for a cellular CDMA system that operates in an environment whose delay spread is less than the period of the sequences. Without the bandlimiting effect, such a system is free from ISI and multiple access interference (MAI) that limit the system capacity.

Our main interest is to find proper training sequences for use in a preamble so that a MIMO-OFDM receiver can easily accomplish the link setup process within the preamble period. The setup process includes at least package detection, frame and frequency synchronization and channel estimation. Such a synchronization procedure involves the detection and estimation of some signal and channel parameters in a multiple antenna scenario. Conventional maximum likelihood (ML) paradigm solves this data-aided estimation and detection problem by an estimator-correlator type receiver structure and necessitates the ideal AC and CC properties on the part of the training sequences. As will become clear in the next section that one can not have both ideal AC and CC properties. The next best thing one can have is something similar to the PS sequences,

assuming a known delay spread channel. In that situation we can employ the PS sequences, using different members of the family in different transmit antennas during the preamble period. To remove the constraint on the PS sequence length, we propose a new family of sequences which have similar AC and CC behavior. Instead of using the ad hoc approach of [3], we interpret the AC and CC requirements in the transform domain and provide a simpler and more natural derivation. We offer a new simple derivation of the PS family and show that the new family of sequences is a generalization of the PS sequences.

2.1 Welch bound (Sarwate bound)

Sets of periodic sequences with good correlation properties are desired in many communication applications. Oftentimes we hope to have a set of sequences whose AC function has a single peak at the zero delay and whose CC values are identically zero. Such sequences can be used to avoid or minimize the interference from other antennas (or other users) and eliminate the ISI due to a multi-path channel. However, it is observed that a set of sequences having good AC properties, e.g., PN sequences and Gold sequences, does not have good CC properties. On the other hand, the ideal AC requirement can not be met if the set has good CC properties. Walsh-Hadamard code is a typical example. In fact the bounds on CC and AC of sequences derived in [4] and [5] indicate that there is a tradeoff between AC and CC when designing sequences. For convenience of reference we present these bounds in the followings.

Theorem 1 *Let X denote a set of K complex-valued sequences of period N, i.e., for every sequence $u \in X$, $u_i = u_{i+N}$, for all $i \in \mathbf{Z}$, $\mathbb{Z}$ being the set of integers. The periodic CC function $\theta(u, v)(\cdot)$ for sequences u, $v \in X$ is defined by*

$$\theta(u, v)(l) = \sum_{i=0}^{N-1} u_i v_{i+l}^*, \quad l \in \mathbb{Z}, \tag{2.1}$$

where and a^* denotes the complex conjugate of a.

The periodic AC function $\theta(u)(l)$ for the sequence u is just $\theta(u,u)(l)$. We assume that $\theta(u)(0) = N$ for all $u \in X$ then it is obvious that $|\theta(u)(l)| \leq N$ and $|\theta(u,v)(l)| \leq N$ for all $u, v \in X$. For the set X, the maximum periodic CC magnitude θ_c, and the maximum out-of-phase periodic AC magnitude θ_a defined by

$$\begin{aligned} \theta_c &= \max\{|\theta(u,v)(l)| : u, v \in X, u \neq v, 0 \leq l \leq N-1\} \\ \theta_a &= \max\{|\theta(u)(l)| : u \in X, 0 < l \leq N-1\} \end{aligned}$$

must satisfy

Theorem 2 *For any set X of K sequences of period N satisfying $\theta(u)(0) = N$ for all $u \in X$,*

$$\left(\frac{\theta_c^2}{N}\right) + \frac{N-1}{N(K-1)}\left(\frac{\theta_a^2}{N}\right) \geq 1. \tag{2.2}$$

The proof was given in [5]. Invoking this theorem, we assign properly-selected sequences with period $N (N \geq 2)$ to different transmit antennas. For a MIMO receive it is necessary to separate signals emitting from different transmitting antennas, or equivalently, it should have the capability to resolve and estimate the impulse response of each sub-channels between any pair of transmit-receive antennas. One way to achieve near-optimal channel estimation is to use pilot sequences that have perfect CC properties, i.e., $\theta_c = 0$. If there are K transmit antennas, we need at least K different preamble sequences. The above theorem implies that $\theta_a \geq N\sqrt{\frac{K-1}{N-1}}$ and, for a MIMO system with two transmit antennas ($K = 2$), we have $\theta_a \geq \frac{N}{\sqrt{N-1}} \geq \sqrt{N}$. Thus even for a set of only two sequences of length N with perfect CC properties, i.e., $\theta_c(l) = 0$ for all l, it is impossible for them to yield the ideal AC function $\theta_a(n) = 0$. If we use these sequences as the training signals in the system, the received signal will be interfered by their delay versions in a multi-path environment. The above discussion convince us that instead of trying to find a set of sequences with ideal correlation properties, we might as well focus our attention on finding some set of sequences that have nonzero AC values at

some desired positions n's whose corresponding AC values $\theta(u)(n) = n_l \neq 0$ meet our requirements.

2.2 A new set of orthogonal sequences

In this section, we present a new set of sequences having some desired periodic AC and CC properties. This new family of sequences is a generalized version of what had been referred to as the PS sequences [3]. Notations and definitions are given first and then a class of sequences to be used to generate the new family is introduced before presenting the derivation of the new sequences and the associated properties.

2.2.1 Notation and definitions

Definition 1 *Let us define the $N \times N$ DFT matrix with index m as*

$$F^{(N,m)}(k,l) = [W_N^{-klm}] = (W_N^m)^{-kl}, \tag{2.3}$$

where m is a natural number, $k, l = 0, 1, \ldots, N-1$, $W_N = e^{j2\pi/N}$ and $j = \sqrt{-1}$.

Definition 2 *The diagonalized matrix $D(\{x_l\})$ associated with the sequence $\{x_l\}$ is defined as*

$$D(\{x_l\}) = diag(\{x_l\}). \tag{2.4}$$

Definition 3 *The quotient and residual functions Q and R corresponding to the devisee and divisor (α, β) are defined as*

$$Q(\alpha, \beta) = q, \quad R(\alpha, \beta) = r, \tag{2.5}$$

where α and q are integers, β is a natural number, and $\alpha = q\beta + r$ with $r = 0, 1, \ldots, \beta - 1$.

The above definitions are adopted from [3] for convenience of comparison.

2.2.2 FZC sequences

The well-known complex sequences, Frank-Zadoff-Chu (FZC) sequences [6], [7] render a Dirac-like periodic AC functions whose values are zeros for all non-zero lags. More specifically, a FZC sequence $\{a_k\}$ of length N has entries of unity-modulus complex numbers, i.e., $a_k = e^{j\alpha_k}, k = 0, \ldots, N-1$. When N is even, they are given by

$$a_k = \exp\left(j\frac{M\pi k^2}{N}\right), \tag{2.6}$$

where M is an integer prime to N, while if N is odd,

$$a_k = \exp\left(j\frac{M\pi k(k+1)}{N}\right), \tag{2.7}$$

where M is also an integer prime to N. It is proved that for any such length N sequence, $\theta(a)(n) = N\delta(n)$, for $n = 0, 1, \ldots, N-1$. The single maximum of magnitude N occurs at $n = 0$.

2.2.3 Generation of the new set of sequences

We now introduce a procedure to generate a family of sequences of length $N = KN_c$ based on the FZC code. To begin with, we need a length-N_c sequence having perfect AC property, i.e., the AC function of this sequence is zero for all non-zero delays. This sequence will be refer to as the basis or the generating sequence henceforth. FZC sequence is a good candidate that meets our need. Denote the FZC code of length N_c by the N_c-by-1 vector $\vec{x}$ and let $\vec{c}_0, \vec{c}_1, \ldots, \vec{c}_{K-1}$ be the sequences to be generated which have the desired AC and CC properties with the vector $\vec{c}_i$ being the ith sequence of length N.

Taking the N_c-point DFT of the vector $\vec{x}$, we obtain

$$X(k) = \sum_{n=0}^{N_c-1} x_i W_{N_c}^{kn}, W_{N_c} = e^{-j2\pi/N_c}, \text{ and } 0 \le k < N_c. \tag{2.8}$$

The N-DFT of the vector $\vec{c}_i$ is

$$C_i(\lambda) = \sum_{n=0}^{N-1} c_i W_N^{\lambda n}, W_N = e^{-j2\pi/N}, \text{ and } 0 \le \lambda < N. \tag{2.9}$$

Using following assignments on $C_i(\lambda)$ and λ

$$C_i(\lambda) = \begin{cases} KX(k) & ; \quad \lambda = Kk + i, \\ 0 & ; \quad \text{otherwise}, \end{cases} \tag{2.10}$$

and taking the N-point IDFT on $C_i(\lambda)$, we obtain a set of sequences of length N. This procedure is illustrated in Fig. 2.1.

2.2.4 Properties of the new set of sequences

1. *Autocorrelation function:*

Let $c_{l,i}$ represents the lth element in the sequence vector $\vec{c}_i$. The AC function of the new sequence $\vec{c}_i$ is given by

$$\begin{aligned} \theta(c_i)(n) &= \sum_{l=0}^{N-n-1} c_{l+n,i} c_{l,i}^* + \sum_{l=N-n}^{N-1} c_{l+n-N,i} c_{l,i}^* \\ &= NW_N^{ni} \delta(R(n, N_c)) \end{aligned} \tag{2.11}$$

Before proving the AC function above, we need introduce some simple lemmas:

Lemma 1 *The periodic autocorrelation function of $x(n)$, $\theta(x,x)(n)$, is equivalent to the circular convolution function between $x(n)$ and $x^*(-n)$.*

Proof:

The periodic autocorrelation function of a sequence of length N, $\{x(n)\}$, is defined as $\theta(x,x)(n) \triangleq \sum_{\tau=0}^{N-1} x(n+\tau)x^*(\tau)$. The circular convolution function between $x(n)$ and $x^*(-n)$ is

$$\begin{aligned} x(n) \circledast x^*(-n) &= \sum_{\tau=0}^{N-1} x(n-\tau)x^*(-\tau) \\ &= \sum_{\tau=0}^{N-1} x(n+\tau)x^*(\tau) \\ &= \theta(x,x)(n) \end{aligned} \tag{2.12}$$

Using the same argument, we conclude that the cross-correlation function $\theta(x,y)(n)$ is equivalent to $x(n) \circledast y^*(-n)$.

Lemma 2 *For any two sequences $x(n), y(n)$ with perfect CC property, i.e., $\theta(x,y)(n) = 0$ for all integer n, their DFT's must satisfy*

$$X[k]Y[k] = 0, \ \forall \ \ k.$$

Proof:

Perfect CC function implies $\theta(x,y)(n) = 0$ for all n, or equivalently, as implied by Lemma 1, $x(n) \circledast y^*(-n) = 0$. Taking DFT on both sides, we have $X[k]Y^*[k] = 0$.

Proof of (2.11)

Lemma 1 implies that the AC function for $\vec{c_i}$ is given by

$$\theta(c_i, c_i)(n) = c_i(n) \circledast c_i^*(-n). \tag{2.13}$$

Taking N-point DFT on both side, we have

$$\Theta_{c_i,c_i}(\lambda) = C_i(\lambda)C_i^*(\lambda), \quad 0 \le \lambda < N. \tag{2.14}$$

Substituting (2.10) into (2.14), $\Theta_{c_i,c_i}(\lambda)$ can be expressed as:

$$\Theta_{c_i,c_i}(\lambda) = \begin{cases} K^2 X(k)X^*(k) & ; \ \lambda = Kk + i, \\ 0 & ; \ \text{otherwise}, \end{cases} \tag{2.15}$$

where $X(k)$'s ares the N_c-point DFTs of the FZC sequence $\vec{x}$ which is of length N_c. Since $\vec{x}$ is an FZC sequence, the AC function of $\vec{x}$ is

$$\theta(x,x)(n) = x(n) \circledast x^*(-n) = N_c\delta(n). \tag{2.16}$$

Taking N_c-point DFT on (2.16), we have

$$\Theta(x,x)(k) = X(k)X^*(k) = N_c. \tag{2.17}$$

Comparing (2.15) and (2.17), we find out that $\Theta_{c_0,c_0}(\lambda)$ is an rate-expanded version of $\Theta(x,x)(k)$, and K is the expanding rate. That is,

$$\Theta_{c_0,c_0}(\lambda) = \begin{cases} K^2\Theta(x,x)(k) = K^2 N_c & ; \ \lambda = Kk, \\ 0 & ; \ \text{otherwise}. \end{cases} \tag{2.18}$$

Hence we can expect that the AC function of the newly generated sequence $\vec{c}_0$ be periodic with period N_c, i.e.,

$$\theta_{c_0,c_0}(n) = N\delta(R(n, N_c)), \tag{2.19}$$

where $R(\cdot)$ is defined in (2.5). The other $\Theta_{c_i,c_i}(\lambda)$'s for $0 < i < K$ are simply frequency-shifting functions of $\Theta_{c_0,c_0}(\lambda)$, i.e.,

$$\Theta_{c_i,c_i}(\lambda) = \Theta_{c_0,c_0}(\lambda - i). \tag{2.20}$$

Fig. 2.2 gives a graphic explanation on this relation. The frequency-shifting operation induces a phase rotation in time-domain. This means that

$$\theta_{c_i,c_i}(n) = W_N^{ni}\theta_{c_0,c_0}(n) = NW_N^{ni}\delta(R(n, N_c)), \tag{2.21}$$

where W_N is defined by $e^{j2\pi/N}$ as before. The AC function has a nonzero value only when $R(n, N_c) = 0$; i.e., $n = IN_c$, where I is an integer. One can control the interval (period of the AC function) by choosing the value of N_c properly. Fig. 2.3 is a typical plot for the AC function of the new sequences. In this example, the sequence length is $N = KN_c = 2 \times 32$.

2. *Crosscorrelation function:*

Let us denote two new sequences as $\vec{c}_i$ and $\vec{c}_j$. The CC function of the two sequences is 0 if $i \neq j$.

Proof:

From (2.15), we have $\forall\lambda$,

$$\Theta_{c_i,c_i}(\lambda)\Theta_{c_j,c_j}(\lambda) = 0, \text{ for } i \neq j, \text{ and } 0 \leq i, j < K. \tag{2.22}$$

Substituting (2.14) into the equation above, we have:

$$C_i(\lambda)C_i^*(\lambda)C_j(\lambda)C_j^*(\lambda) = 0, \text{ for } i \neq j, \text{ and } 0 \leq i, j < K. \tag{2.23}$$

It implies that

$$\Theta_{c_i,c_j}(\lambda)\Theta_{c_i,c_j}^*(\lambda) = 0, \text{ for } i \neq j, \text{ and } 0 \leq i, j < K. \tag{2.24}$$

Hence $\Theta_{c_i,c_j}(\lambda) = 0$ for all λ. By applying Lemma 1 and Lemma 2, we conclude that, for $i \neq j$, $\theta(c_i, c_j)(n) = 0$ for all n. Hence they do have perfect CC properties.

The new set of sequences can be used as the training sequences for MIMO-OFDM systems. The parameters K and N_c of the sequences are to be determined by the number of transmit antennas and the length of the maximum delay spread.

2.2.5 Summary of the new set of sequences

The major attributes of the proposed family of sequences are :

1. Sequence are composed of complex numbers with unity magnitude.

2. The basis sequence determines the AC function in one period, and the CC properties between sequences are determined by their DFTs.

3. Given a sequence of length N_c with the perfect periodic AC property, we generate K different sequences of length KN_c; all of them have periodic impulse-like AC function.

2.3 PS Sequences

In [3], a new class of polyphase sequences (called *PS sequences*) for CDMA systems and its generation method are suggested. The PS sequence is of length N_s, where $N_s = KN_b^2$. The value K determines how many different sequences having excellent CC function we can used. The value N_b^2 determines the period of the AC function of the sequences. The PS sequences have perfect CC function so we can completely reject the interference from other users in a multiuser system with these sequences. However, the PS sequence still has some unwanted peaks in its AC function. It degrades the system performance when the system is operated in a multi-path environment. Hence there is a restriction in using the PS sequence in CDMA systems. The delay spread of the reverse-link channels must be small. In this section, we will introduce the PS sequence and its generation methods.

2.3.1 Generation of the PS sequence

Define the basic symbols as N_b (not necessarily distinct) symbols b_i, $i = 0, \ldots, N_b - 1$, all with equal magnitude. Without loss of generality, we assume b_i's are all located on the unit circle in the complex plane. We first generate an orthogonal sequence from b_i's. Simply take $\{W_{N_b}^0, \ldots, W_{N_b}^{N_b-1}\}$(uniformly distributed on the unit circle) as a set of basic symbols. For a set of basic symbols $\{b_i\}$ and $1 \leq m \leq N_b - 1$, we define the basic orthogonal sequence matrix G of size $N_b \times N_b$ as

$$G = F^{(N_b,-m)} D(\{b_i\}). \tag{2.25}$$

The basic orthogonal sequence $\{g_p\}$ of length N_b^2 is defined by [8]

$$g_p = G_{Q(p,N_b),R(p,N_b)} \tag{2.26}$$

or equivalently, if $\vec{g} = [g_0, g_1, \ldots, g_{N_b^2-1}]^T$,

$$\vec{g} = \mathrm{vec}(G^T), \tag{2.27}$$

where $\mathrm{vec}(\cdot)$ denotes the stacking operator.

Using the basic orthogonal sequence $\{g_p\}$, we form the $N_s \times K$ matrix H as

$$H = [h_{i,k}], \tag{2.28}$$

where

$$h_{i,k} = \sum_{p=0}^{N_b^2-1} g_p \delta(i - k - pK), \tag{2.29}$$

$N_s = KN_b^2$, $\delta(n) = \begin{cases} 1, & n = 0 \\ 0, & n \neq 0 \end{cases}$, and K is a natural number.

The *PS sequence matrix* C of size $N_s \times K$ (or $KN_b^2 \times K$) is defined as

$$C = [c_{l,k}] = \frac{1}{N_b} F^{(N_s,-1)} H. \tag{2.30}$$

Each column vector of C forms a sequence $\{c_{l,k}, l = 0, 1, \ldots, N_s - 1\}$ which is called a *PS sequence*.

2.3.2 Properties of the PS sequences

1. *Autocorrelation function:*

The AC function of the PS sequence is given by

$$\begin{aligned}\theta(c)(\tau) &= \sum_{l=0}^{N_s-\tau-1} c_{l+\tau,k}c_{l,k}^* + \sum_{l=N_s-\tau}^{N_s-1} c_{l+\tau-N_s,k}c_{l,k}^* \\ &= N_s W_{N_s}^{\tau k}\delta(R(\tau, N_b^2)). \end{aligned} \tag{2.31}$$

The AC function has a nonzero value only when $R(\tau, N_b^2) = 0$; i.e., $\tau = IN_b^2$, where I is an integer. We can control the interval or period by properly choosing the value of N_b^2. On the contrary, the PN sequence has nonzero values of the AC function at all intervals. The PS sequence has better CC properties than the PN sequence. Fig. 2.4 is a typical plot for the AC function of the PS sequences.

2. *Crosscorrelation function:*

Let us denote two PS sequences as $\{c_{l,k^I}\}$ and $\{c_{l,k^{II}}\}$. The CC function of the two sequences is 0 if $k^I \neq k^{II}$.

2.4 Comparison

If we compare the proposed sequences with PS sequences, we can find that the main difference between them is the choice of the basic orthogonal sequence. From (2.25) to (2.27), a sequence of length N_b^2 with perfect AC function is generated. This step is similar to generating a FZC sequence of length N_b^2 in our procedure. (This sequence may be not the same with the sequence generated by (2.25), (2.26), and (2.27).) In fact, the only constraint on the basis sequence is its AC property only. We can generate a family of PS-like sequences as soon as we find a sequence with perfect AC function. Comparing to the PS sequences, our new sequences have less constraint on sequence length. Fig. 2.3 represents a typical plot for the AC function of the new sequences whose length is $N = KN_c = 2 \times 32$. Notice that we cannot generate PS sequences having the same AC

function as Fig. 2.3, since $32 \neq N_b^2$, for any natural number N_b. We can also apply the new concept discussed in section 2.2.4 to show why the sequence generated from (2.25), (2.26), and (2.27) must be an orthogonal sequence. In chapter 3, we will explain it in another point of view, which is different from what had been discussed in [8]. And from (2.28) to (2.30), these steps are equivalent to the realization described in Fig. 2.2, such that perfect CC properties can be obtained. However we give a much easier proof for CC properties instead of the proof in the [3].

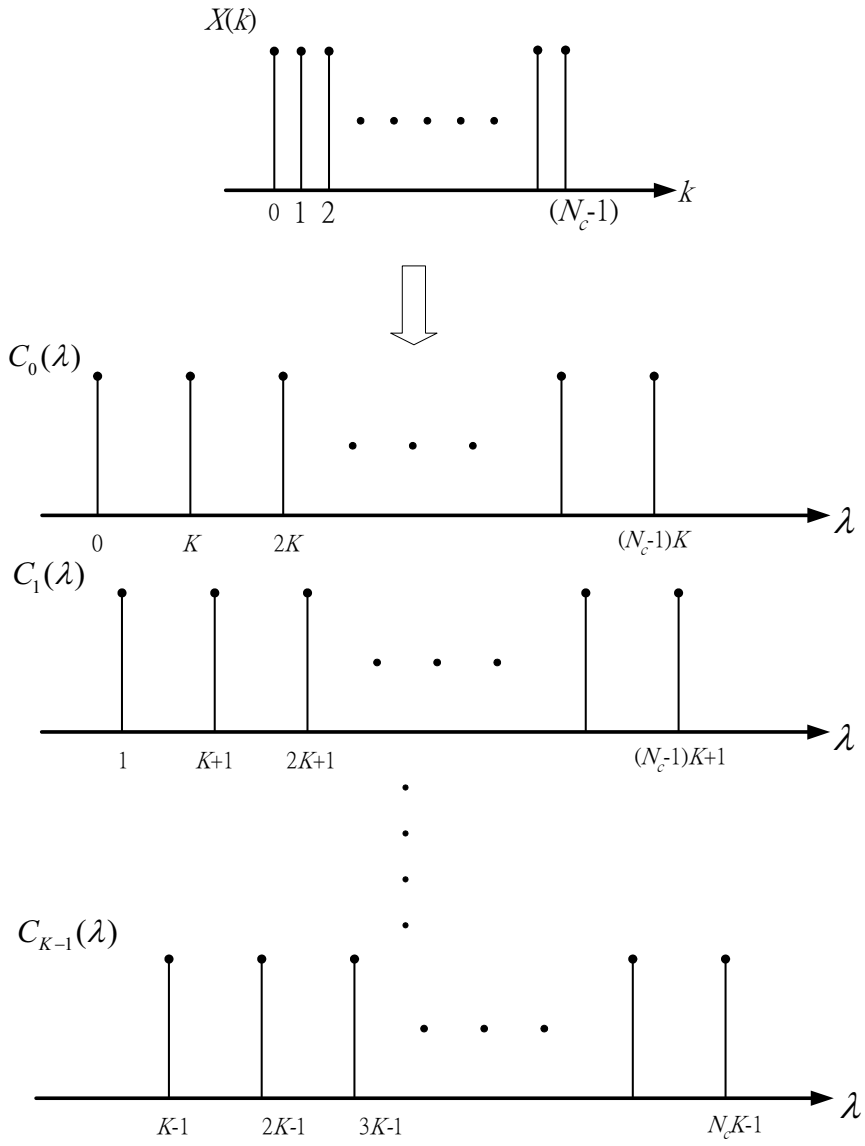

Figure 2.1: Construct the $C_i(\lambda)$'s from the DFT points of the basis sequence.

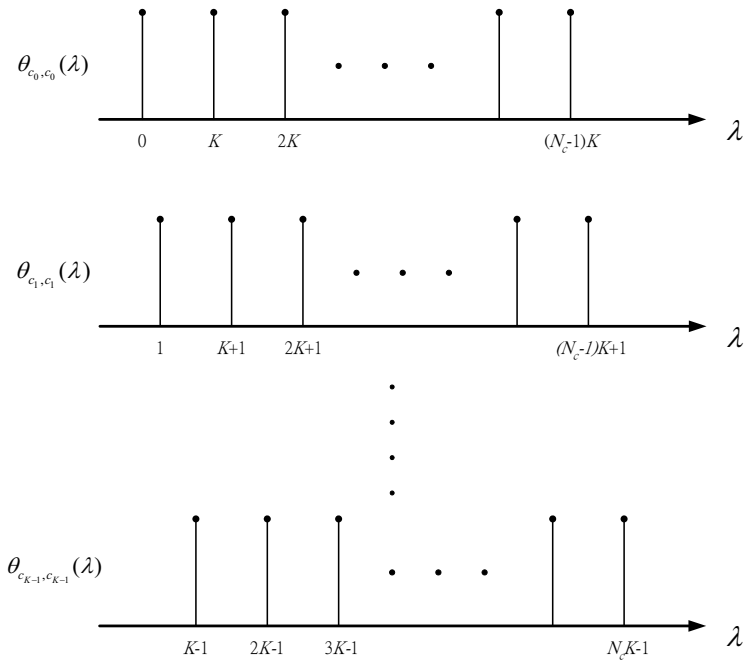

Figure 2.2: $\Theta_{c_i,c_i}(\lambda)$'s for $0 < i < K$ are simply frequency-shifting functions of $\Theta_{c_0,c_0}(\lambda)$.

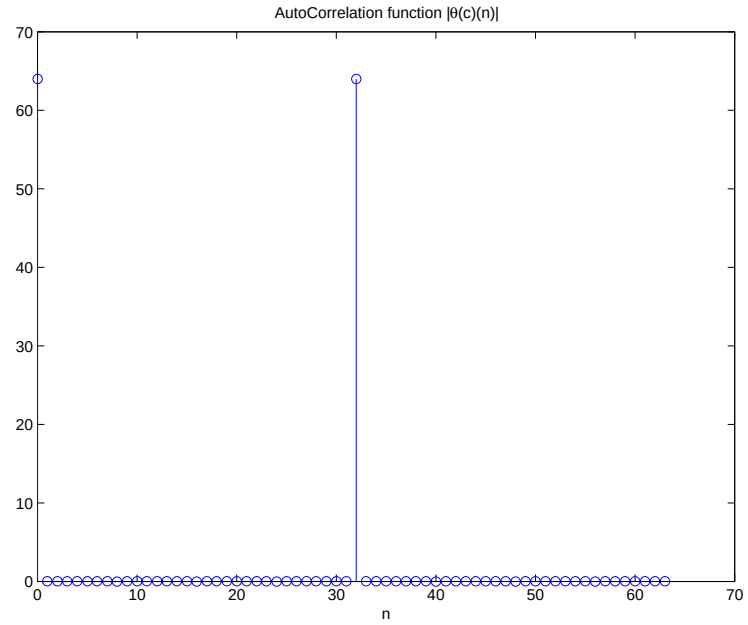

Figure 2.3: The autocorrelation function of the new sequence.($K = 2, N_c = 32$, and $N = KN_c = 64$)

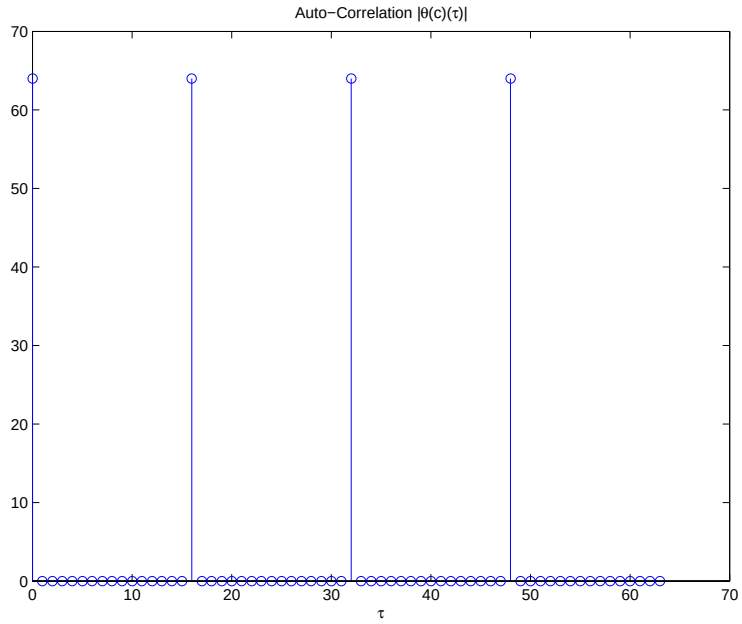

Figure 2.4: The autocorrelation function of the PS sequence.($K = 4, N_b^2 = 16$, and $N_s = KN_b^2 = 64$)

Chapter 3

The Basis Sequence of the PS Sequences

3.1 Preliminary

In the last chapter, we have shown that the PS sequences are generated by a basis sequence with perfect AC property. One of the candidate basis sequences was that presented in [8]. We will demonstrate that one can use the technique similar to that discussed in Chapter 2 to explain why the sequences of [8] have perfect AC function.

For a set of basic symbols $\{b_i\}$ located on the unit circle ($|b_i| = 1$), $0 \leq m \leq N_b - 1$, we define the basic orthogonal sequence matrix G of size $N_b \times N_b$ as

$$G = F^{(N_b,-m)} D(\{b_i\}), \tag{3.1}$$

where $F^{(N,m)}(k,l) = [W_N^{-klm}] = (W_N^m)^{-kl}$, $0 \leq k,l < N$, and $W_N = e^{j2\pi/N}$. Hence $F^{(N,1)}\vec{x}$ is equivalent to the DFT of the time-domain vector $\vec{x}$, and $F^{(N,-1)}\vec{y}$ is equivalent to the IDFT of the frequency-domain vector $\vec{y}$ if the constant factor $1/N$ is omitted. In the following discussion, we will omit the $1/N$ factor since it does not affect the AC property. The basis sequence used in PS sequences is given by:

$$\vec{g} = \mathrm{vec}(G^T), \tag{3.2}$$

where $\mathrm{vec}(\cdot)$ denotes the stacking operator. Here we give a more meaningful interpretation about that why the sequence generated in this way will have perfect periodic AC function under some conditions.

3.2 Generating basis sequences

We take the case for $N_b = 3$ as an example without loss of generality. Assume $m = 1$, then:

$$G = F^{(N_b,-1)} D(\{b_i\}) = F^{(N_b,-1)} \left[\begin{array}{ccc} \vec{b}_0 & \vec{b}_1 & \vec{b}_2 \end{array} \right], \tag{3.3}$$

where $\vec{b}_0 = [b_0\ 0\ 0]^T$, $\vec{b}_1 = [0\ b_1\ 0]^T$, and $\vec{b}_2 = [0\ 0\ b_2]^T$. The ith column vector of the matrix G, $\vec{g}_i$, is equal to the N_b-IDFT of $\vec{b}_i$. Since there is only one non-zero element in the vector $\vec{b}_i$ and the elements in F are all of unit magnitude, the elements of $\vec{g}_i$ must have identical magnitude. In order to make the explanation clear, we denote

$$G = [\vec{g}_0\ \vec{g}_1\ \vec{g}_2] = \left[\begin{array}{ccc} g_0 & g_3 & g_6 \\ g_1 & g_4 & g_7 \\ g_2 & g_5 & g_8 \end{array} \right]. \tag{3.4}$$

The relation between b_i's and g_i's is showed in Fig. 3.1. We proceed by invoking a

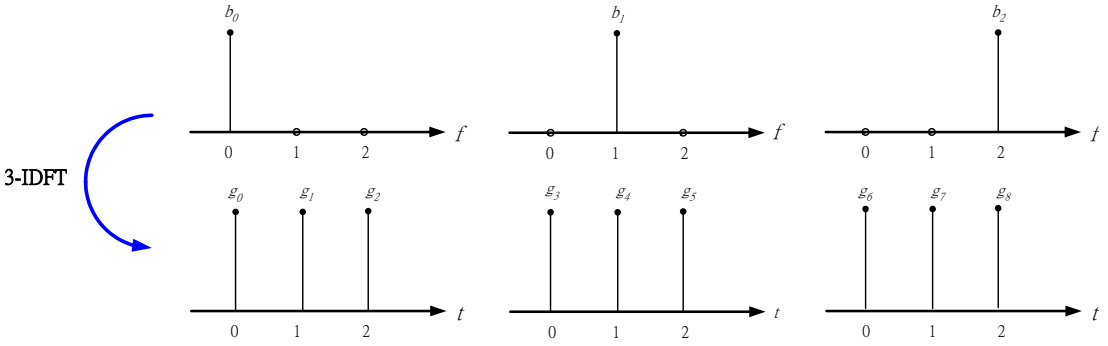

Figure 3.1: 3-IDFT of $\vec{b}_i$. The elements of the matrix G, $g_0 \sim g_8$, are complex number with unit magnitude.

technique similar to (2.15). Performing the rate expanding on the time-domain vectors $\vec{g}_0$, $\vec{g}_1$, and $\vec{g}_2$ by inserting some zeros with an expanding rate of $N_b = 3$, we obtain the expanded vectors ($N_b^2 \times 1$)

$$\vec{g}_{e0} = [\ g_0\ 0\ 0\ g_1\ 0\ 0\ g_2\ 0\ 0\ ]^T \tag{3.5}$$

$$\vec{g}_{e1} = [\ g_3\ 0\ 0\ g_4\ 0\ 0\ g_5\ 0\ 0\ ]^T \tag{3.6}$$

$$\vec{g}_{e2} = [\ g_6\ 0\ 0\ g_7\ 0\ 0\ g_8\ 0\ 0\ ]^T. \tag{3.7}$$

After taking N_b^2-DFT on the expanded vectors(sequences), the corresponding frequency-domain sequences will repeat periodically. Then we do some time-shifting on $\vec{g_{e1}}$ and $\vec{g_{e2}}$ such that there is no overlapping if we sum $\vec{g_{e0}}$, $\vec{g_{e1}}$, and $\vec{g_{e2}}$ together. Denote the time-shifted vectors as $\vec{g_{es0}}$, $\vec{g_{es1}}$, and $\vec{g_{es2}}$, and then

$$\vec{g_{es0}} = [\ g_0 \quad 0 \quad 0 \quad g_1 \quad 0 \quad 0 \quad g_2 \quad 0 \quad 0\ ]^T \tag{3.8}$$

$$\vec{g_{es1}} = [\ 0 \quad g_3 \quad 0 \quad 0 \quad g_4 \quad 0 \quad 0 \quad g_5 \quad 0\ ]^T \tag{3.9}$$

$$\vec{g_{es2}} = [\ 0 \quad 0 \quad g_6 \quad 0 \quad 0 \quad g_7 \quad 0 \quad 0 \quad g_8\ ]^T. \tag{3.10}$$

This shifting operation will cause some phase rotation in frequency-domain. In fact the phase rotation is not important, and we will show the reason later. We depict these steps in Fig. 3.2 in which the phase rotation effects are also shown.

Summing the vectors $\vec{g_{es0}}$, $\vec{g_{es1}}$, and $\vec{g_{es2}}$ together, we obtain

$$\vec{g} = \vec{g_{es0}} + \vec{g_{es1}} + \vec{g_{es2}} = \mathrm{vec}(G^T). \tag{3.11}$$

We plot the corresponding result in Fig. 3.3. The corresponding N_b^2-DFT points of $\vec{g}$ are all with the same magnitude.

In order to explain the effects of the phase rotation, we need to recall some properties introduced in chapter 2. Denote the AC function of a sequence $x(n)$ as $\theta(x,x)(n)$ and its N_c-DFT as $\Theta(x,x)(k)$, we hope that

$$\theta(x,x)(n) = N_c\delta(n), \tag{3.12}$$

and

$$\Theta(x,x)(k) = X(k)X^*(k) = N_c. \tag{3.13}$$

These two equations had been mentioned in (2.16) and (2.17). Hence if we set $X(k) = \sqrt{N_c}e^{j\phi_k}$, i.e., all frequency components have the same magnitude, then (3.13) can be achieved. The constant $\sqrt{N_c}$ can be ignored since it does not affect the AC and CC properties. Notice that there is no constraint on the choice of $\{\phi_k\}$. We can conclude

that a sequence has perfect periodic AC property if all of its frequency components have the same magnitude. Hence the new sequence $\vec{g}$ has perfect AC property. This statement also explains why the phase rotation induced from the time-shifting operation is not important. From Figs. 3.2 and 3.3, we also can get the idea why the transpose and the stacking operations in (3.2) are needed. Up to now, we have concentrate our

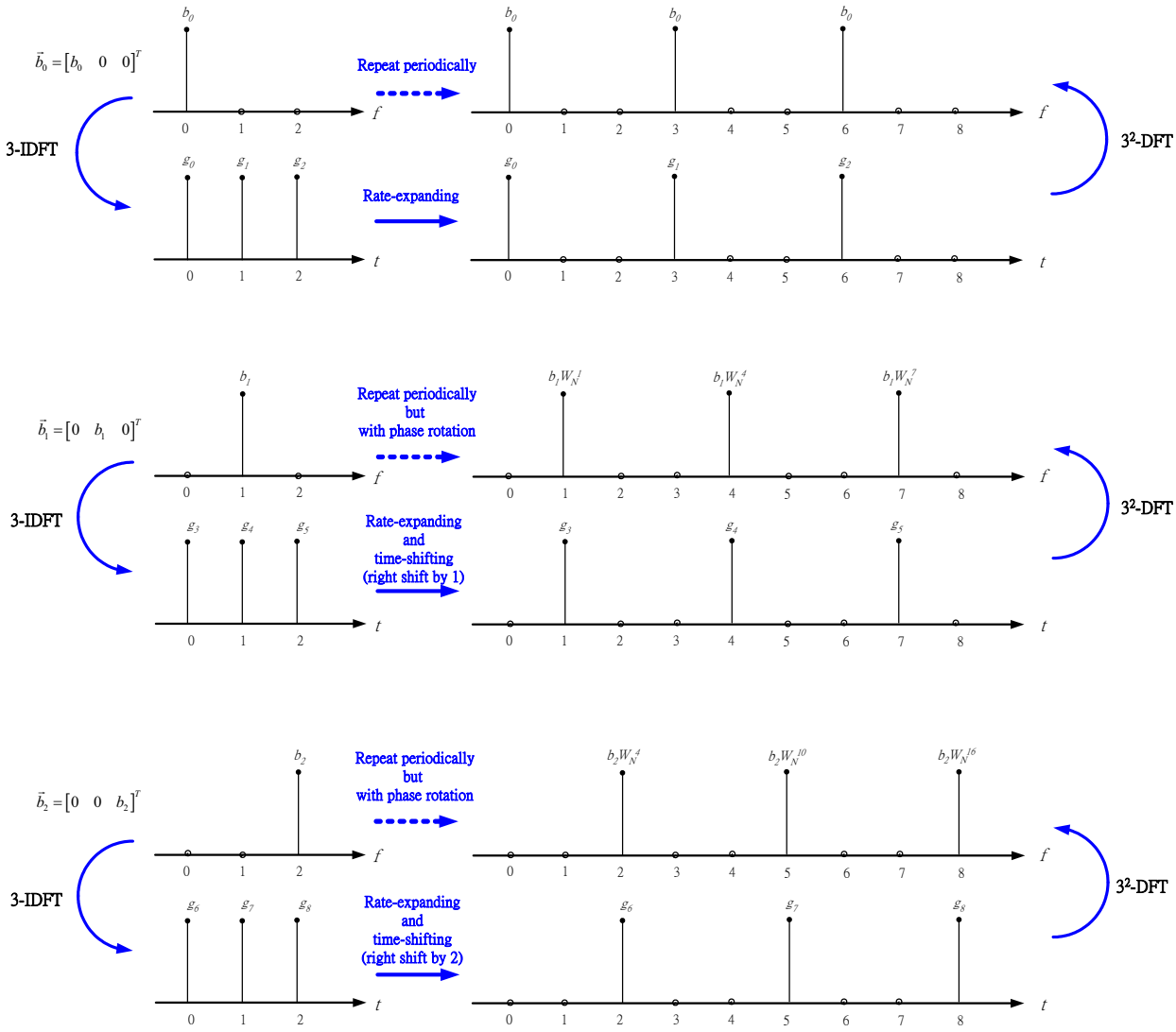

Figure 3.2: Rate-expanding and time-shifting. The time-domain sequences and their corresponding frequency-domain sequences are showed.

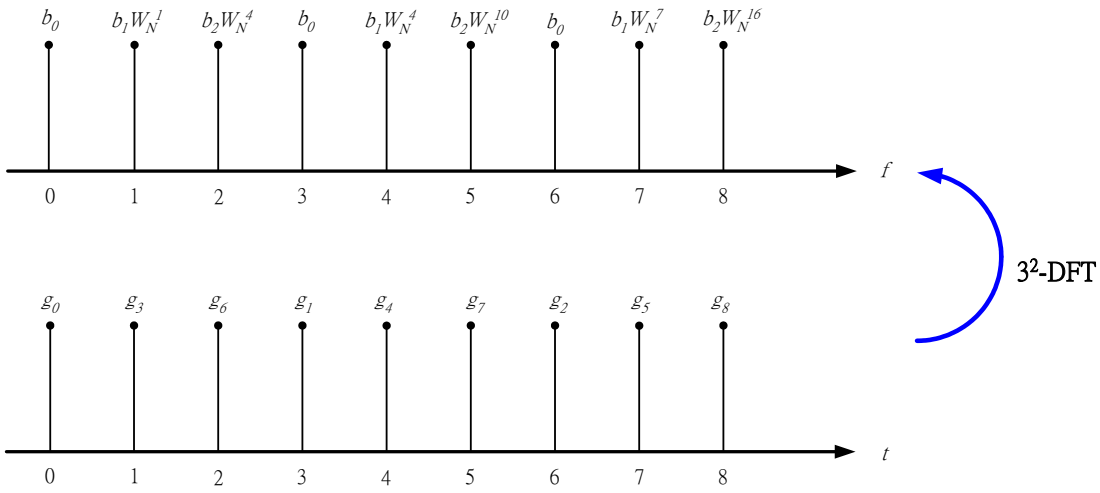

Figure 3.3: Generate the new sequence with perfect periodic AC property. All frequency components are of equal magnitude.

discussion on the case $m = 1$ only. The case $m \neq 1$ is the subject of our next discourse. We need to re-define some notations.

Let $X_i(k) = b_i\delta(k-i)$, then $[X_i(0),\ X_i(1),\ \ldots,\ X_i(N_b-1)]^T = \vec{b}_i$. Taking N_b-point IDFT on $X(k)$'s, we get a sequence $x_i(n)$, for $0 \leq n \leq N_b-1$, and $[x_i(0),\ x_i(1),\ \ldots,\ x_i(N_b-1)]^T = \vec{g}_i^{(m=1)} \triangleq \vec{g}_i^{(1)}$. This is equivalent to the case discussed before for $m = 1$. The ith column vector of the matrix $G^{(m)}$ with $m \neq 1$ can be written as:

$$\vec{g}_i^{(m)} = [x_i^{(m)}(0),\ x_i^{(m)}(1),\ \ldots,\ x_i^{(m)}(N_b-1)]^T, \tag{3.14}$$

where

$$x_i^{(m)}(n) = \sum_{k=0}^{N_b-1} X_i(k)W_{N_b}^{kmn} = b_iW_{N_b}^{imn}. \tag{3.15}$$

For the case that $m = 1$, $x_i^{(1)}(n) = x_i(n) = b_iW_{N_b}^{in}$. We can observe that $x_i^{(m)}(n)$ is a phase-rotated version of $x_i(n)$. Hence we have following relations:

$$x_i(n) \overset{DFT}{\longrightarrow} X_i(k) = b_i\delta(k-i) \quad \Longrightarrow \quad x_i^{(m)}(n) \overset{DFT}{\longrightarrow} X_i[(k-i(m-1))_{N_b}], \tag{3.16}$$

and $X_i[(k-i(m-1))_{N_b}] = b_i\delta[(k-im)_{N_b}]$. For convenience, we will use the notation $(n)_{N_b}$ to denote (n modulo N_b). The term $b_i\delta[(k-im)_{N_b}]$ means that the effect of

different values of m is simply the step size of index shifting in frequency-domain. If we can keep the shifted tones still non-overlapping, the sequence vec$\{{G^{(m)}}^T\}$ can preserve perfect periodic AC property. To change another words, if there are some values of m such that the sequence vec$\{{G^{(m)}}^T\}$ has perfect AC function, then we can find a column-reordered matrix P from the diagonal matrix $D(\{b_i\}) = [\vec{b}_0, \ldots, \vec{b}_{N_b-1}]$, such that $F^{(N_b,-m)}D(\{b_i\}) = F^{(N_b,-1)}P$. The RHS is the case that $m = 1$, which has been discussed. Now we check what the values of m should be such that the shifted tones are still non-overlapping. We consider two cases separately, depending on if m is prime to N_b or not.

Case I *g.c.d.*$(m,\ N_b) = 1$

If there is one tone lapped over another after being shifted, then

$$\begin{aligned} & im \bmod N_b = jm \bmod N_b, \text{ for } i \neq j,\ 0 \leq i, j < N_b. \\ \Rightarrow \quad & (i-j)m \bmod N_b = 0 \\ \Rightarrow \quad & (i-j)m = pN_b,\ p \in \mathbb{Z} \end{aligned} \tag{3.17}$$

The assumption that *g.c.d.*$(m,\ N_b) = 1$ implies that $N_b|(i-j)$, $\therefore\ i = j$. We thus conclude that if there are two tones with $i \neq j$, they will not overlap after shifting.

Example 1 *Consider the case,* $N_b = 4, m = 3, W_4 = e^{j2\pi/4}$, *and* $\vec{b} = \{W_4^1, W_4^2, W_4^3, W_4^4\}$. *In this case we have g.c.d.*$(m,\ N_b) = 1$. *The basic orthogonal sequence matrix* G *is defined by* $F^{(N_b,-m)}D(\{b_i\})$. *Taking DFT on each column vector of* $G^{(m)}$, *we get the column vectors of* P. *The result is shown in Fig. 3.4, and the AC function of the sequence vec*$({G^{(m)}}^T)$ *is plotted in Fig. 3.5.*

Case II *g.c.d.*$(m,\ N_b) = d$:

Let $m = hd$, $N_b = kd$, and $g.c.d.(h, k) = 1$.

$$\begin{aligned} & im \bmod N_b = jm \bmod N_b \\ \Rightarrow \quad & (i-j)hd \bmod kd = 0 \\ \Rightarrow \quad & (i-j)h \bmod k = 0 \\ \Rightarrow \quad & (i-j)h = qk,\ q \in \mathbb{Z} \end{aligned} \tag{3.18}$$

$g.c.d.(h,\ k) = 1 \ \Rightarrow \ k|(i-j) \quad \therefore i = j \bmod k.$

Hence there will be d tones lapped together. We can denote $\{j, j+k, j+2k, \ldots\}$ as a coset. There will be d elements in this coset and one can find N/d different cosets.

From the above discussion we conclude that the sequence vec$\{{G^{(m)}}^T\}$ has perfect periodic AC property if $g.c.d.(m,\ N_b) = 1$.

Example 2 *Consider the case–*$N_b = 4, m = 2, W_4 = e^{j2\pi/4}$, *and* $\vec{b} = \{W_4^1, W_4^2, W_4^3, W_4^4\}$. *In this case we have* $g.c.d.(m,\ N_b) = 2$. *The basic orthogonal sequence matrix* $G^{(m)}$ *is defined by* $F^{(N_b,-m)}D(\{b_i\})$. *Taking DFT on each column vector of vec*$({G^{(m)}}^T)$, *we obtain the desired result as shown in Fig. 3.6. We notice that if we sum up all column vectors, there must be some tones overlapping each other. Hence the AC function will not be perfect; see Fig. 3.7.*

The above discussion indicates that the sequence vec$({G^{(m)}}^T)$ has perfect AC function if $g.c.d.(m,\ N_b) = 1$. Furthermore, if the b_i's are of the same magnitude, the generated sequence will be composed of complex numbers with the same magnitude. Observing Fig. 3.3, we can notice that the elements of the sequence have the same magnitude both in time-domain and frequency-domain. As mentioned before, a sequence has perfect AC function if all of its frequency components have the same magnitude. Hence if we exchange the roles of the "time-domain" sequence and the "frequency-domain" sequence, the AC property still can be maintained. Both the sequence generated in this chapter and the FZC sequence have this property. With this property, the step of (2.10) can be

modified as

$$C_i(\lambda) = \begin{cases} Kx_k & ; \quad \lambda = Kk + i, \\ 0 & ; \quad \text{otherwise.} \end{cases} \tag{3.19}$$

Then the reduced sequence generation procedure is identical to that of the PS sequence.

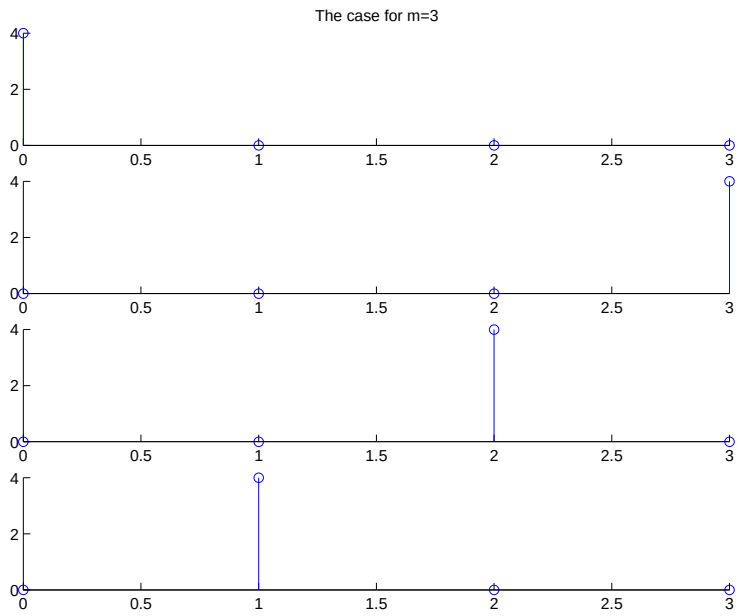

Figure 3.4: $g.c.d.(m,\ N_b) = 1$. Magnitude plot for the DFT of each column vector of $G^{(m)}$.

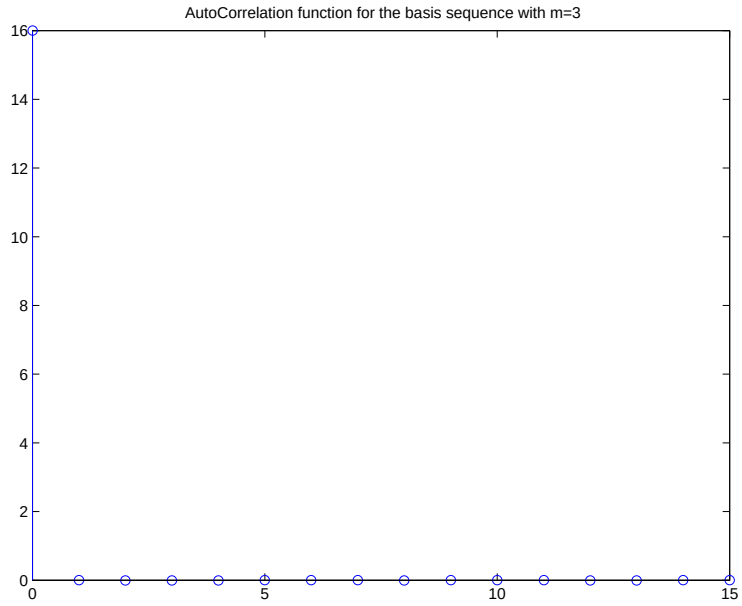

Figure 3.5: $g.c.d.(m,\ N_b) = 1$. AC function of the sequence of $m = 3$.

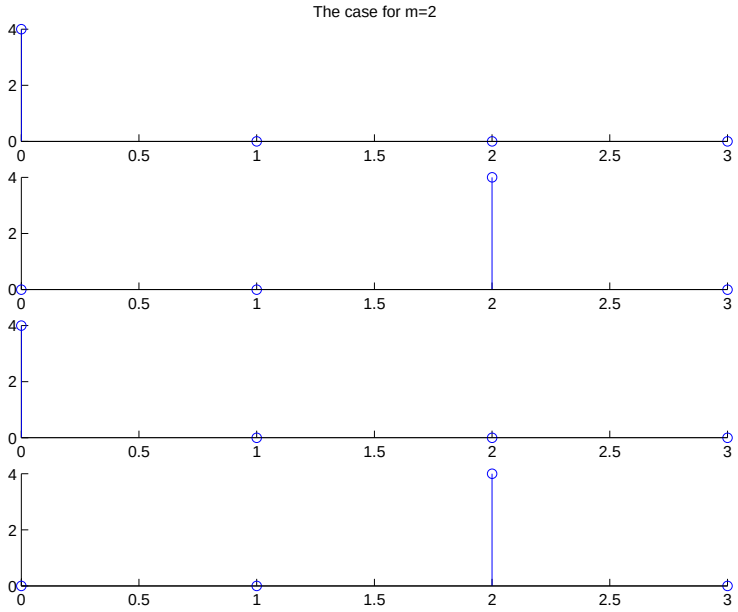

Figure 3.6: $g.c.d.(m,\ N_b) \neq 1$. Magnitude plot for the DFT of each column vector of $G^{(m)}$.

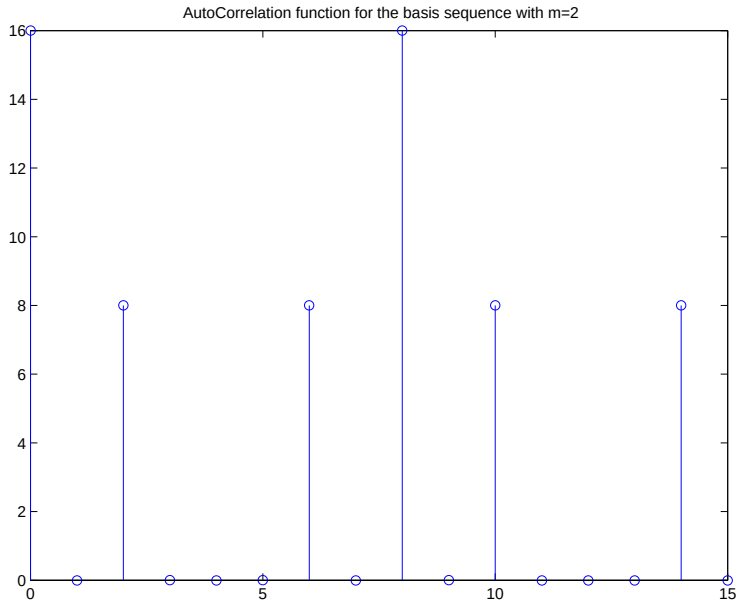

Figure 3.7: $g.c.d.(m,\ N_b) \neq 1$. AC function of the sequence of $m = 2$.

Chapter 4

Multi-dimensional Arrays

Like the one dimensional (1D) case, two dimensional (2D) arrays that possess some desired AC or CC properties are useful in sonar/radar and multimedia applications. Similarly, higher dimensional array signal are needed in some cognitive radio and computer graphics. In this chapter, we extend the concepts developed for one-dimensional sequences to two or higher dimensions cases. The notations and definitions used here follow those of [9].

4.1 Array correlation functions

Let an array sequence $A = a_{i,j}$ be denoted by

$$A = \begin{bmatrix} a_{0,0} & a_{0,1} & \cdots & a_{0,N_2-1} \\ a_{1,0} & a_{1,1} & \cdots & a_{1,N_2-1} \\ \cdots & \cdots & \cdots & \cdots \\ a_{N_1-1,0} & a_{N_1-1,1} & \cdots & a_{N_1-1,N_2-1} \end{bmatrix}. \tag{4.1}$$

The two-dimensional periodic AC function between two array sequences A and B having the same dimensions is defined as

$$R_{A,B}(\phi,\omega) = \sum_{p=0}^{N_1-1} \sum_{q=0}^{N_2-1} a_{p,q} b^*_{p+\phi,q+\omega}. \tag{4.2}$$

An array is called perfect array if its periodic AC function satisfies

$$R_{A,A}(\phi,\omega) = R_A(\phi,\omega) = \begin{cases} E, & (\phi,\omega) = (0,0) \\ 0, & (\phi,\omega) \neq (0,0) \end{cases}, \tag{4.3}$$

where $E = \sum_{p=0}^{N_1-1} \sum_{q=0}^{N_2-1} |a_{p,q}|^2$.

There are many earlier works on the syntheses of perfect arrays. We will apply one of the synthesis methods introduced in [9] to obtain a perfect array. This method is based on

Theorem 3 (Folding method) *Let b_l be a perfect sequence of length $N = N_1 N_2$. Then the array $\{a_{m,n}\}$ defined by*

$$a_{m,n} = b_l,\ m = l \ mod\ N_1,\ n = l \ mod\ N_2 \tag{4.4}$$

is perfect if $gcd(N_1, N_2) = 1$.

4.2 New 2D arrays

To begin with, we need a perfect array sequence. This sequence will be referred to as the basis array. We apply the folding method to the FZC sequence of length $N_1 N_2$, where $gcd(N_1, N_2) = 1$, and then we get an $N_1 \times N_2$ perfect array. Taking the two-dimensional DFT on this basis array, we obtain

$$F(u, v) = \sum_{p=0}^{N_1-1} \sum_{q=0}^{N_2-1} a_{p,q} W_{N_1}^{-pu} W_{N_2}^{-qv}. \tag{4.5}$$

Suppose that the new arrays $C^{(i)}$'s are represented by $K_1 N_1 \times K_2 N_2$ matrices, and their corresponding two-dimensional DFT's are $F^{(i)}(U, V)$ defined by

$$F^{(i)}(U, V) = \sum_{p=0}^{K_1 N_1 - 1} \sum_{q=0}^{K_2 N_2 - 1} c_{p,q}^{(i)} W_{K_1 N_1}^{-pU} W_{K_2 N_2}^{-qV},\quad i = 0, \ldots, (K_1 K_2 - 1). \tag{4.6}$$

We assign $F^{(i)}(U, V)$ according to

$$F^{(i)}(U, V) = \begin{cases} K_1 K_2 F(u, v) & ;\ U = K_1 u + \alpha,\ V = K_2 v + \beta \\ 0 & ;\ \text{otherwise} \end{cases}, \tag{4.7}$$

where $i = K_2 \alpha + \beta,\ 0 \le \alpha < K_1$, and $0 \le \beta < K_2$.

This assignment is illustrated in Fig. 4.1. Taking the two-dimensional IDFT on $F^{(i)}(U, V)$, we obtain an array sequence $C^{(i)}$ of dimension $K_1 N_1 \times K_2 N_2$, where the

two-dimensional IDFT is defined by

$$C^{(i)}(m,n) = \frac{1}{K_1 N_1 K_2 N_2} \sum_{U=0}^{K_1 N_1 - 1} \sum_{V=0}^{K_2 N_2 - 1} F^{(i)}(U,V) W_{K_1 N_1}^{mU} W_{K_2 N_2}^{nV}. \tag{4.8}$$

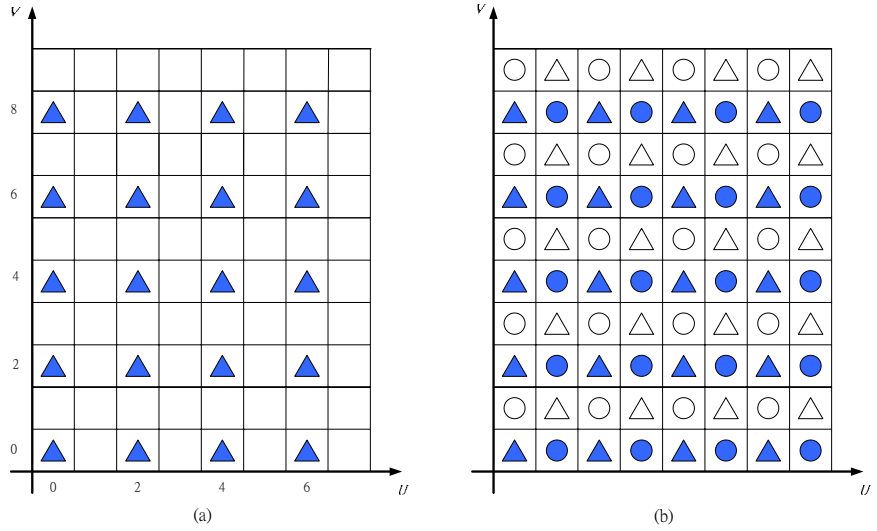

Figure 4.1: (a) Construct the $F^{(0)}(U,V)$ from the two-dimensional DFT points of the basis array. (b) Different symbols represent the non-zero positions of $F^{(i)}(U,V)$ for different i's; ($K_1 = 2$, $K_2 = 2$, $N_1 = 4$, and $N_2 = 5$.)

4.3 Properties of the new proposed 2D arrays

The new array sequences possess some desired properties similar to those in one-dimensional case. The new array sequences $C^{(i)}$'s are of dimension $K_1N_1 \times K_2N_2$. The AC function $|R_{C^{(i)}}(\phi,\omega)|$ is periodic in both arguments–the period in ϕ is N_1 while the period in ω is N_2. The CC function between any two arrays of $C^{(i)}$'s is exactly zero and we can have a family of $K_1 \times K_2$ such array sequences.

Example 3 *Suppose we have a perfect array of dimension $N_1 \times N_2$ already. We can generate K_1K_2 PS-like arrays of dimension $K_1N_1 \times K_2N_2$. Here we set $N_1 = 4, N_2 = 5$, and $K_1 = K_2 = 2$. Applying the folding method to the FZC sequence of length 20,*

we have a 4×5 *perfect array. Denote the FZC sequence as* $\{b_l\}$, $l = 0, \ldots, 19$. *The corresponding perfect array* $\{a_{m,n}\}$ *will be*

$$\begin{bmatrix} b_0 & b_{16} & b_{12} & b_8 & b_4 \\ b_5 & b_1 & b_{17} & b_{13} & b_9 \\ b_{10} & b_6 & b_2 & b_{18} & b_{14} \\ b_{15} & b_{11} & b_7 & b_3 & b_{19} \end{bmatrix}. \tag{4.9}$$

By performing the procedure in the previous section, we can have $K_1 K_2 = 4$ *different PS-like arrays. The magnitude plot of the AC function of these arrays,* $|R_{C^{(i)}}|$, $i = 0, \ldots, 3$, *is shown in Fig. 4.2. The magnitude of the AC function* $|R_{C^{(i)}}(\phi, \omega)|$ *is periodic in both two axes. The period along* ϕ*-axis is* 4, *and the period along* ω*-axis is* 5.

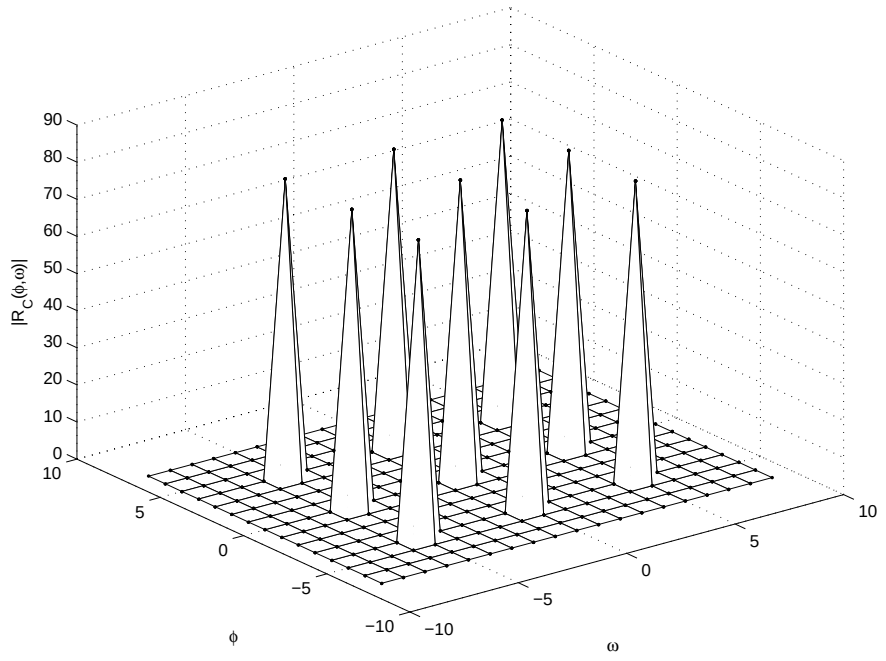

Figure 4.2: Magnitude plot for the two-dimensional periodic AC function of proposed array sequences, $|R_{C^{(i)}}|$. ($K_1 = 2$, $K_2 = 2$, $N_1 = 4$, and $N_2 = 5$.)

4.4 Extension to multi-dimensional arrays

One of the key step in generalizing the technique of section 4.2 to synthesizing multi-dimensional arrays is to find a multi-dimensional perfect array.

Suppose we have an perfect array $\{a_{p_1,p_2,\ldots,p_n}\}$ of dimension $N_1 \times N_2 \times \cdots \times N_n$. Taking n-dimensional DFT on this basis array, we have

$$F(p_1, p_2, \ldots, p_n) = F(\vec{p}) = \sum_{p_1=0}^{N_1-1} \sum_{p_2=0}^{N_2-1} \cdots \sum_{p_n=0}^{N_n-1} a_{p_1,p_2,\ldots,p_n} W_{N_1}^{-p_1 u_1} W_{N_2}^{-p_2 u_2} \cdots W_{N_n}^{-p_n u_n}. \quad (4.10)$$

Suppose that the new arrays $C^{(i)}$'s are $K_1N_1 \times K_2N_2 \times \cdots \times K_nN_n$ matrices, and their corresponding n-dimensional DFT's are $F^{(i)}(P_1, P_2, \ldots, P_n)$:

$$F^{(i)}(P_1, P_2, \ldots, P_n) = F^{(i)}(\vec{P})$$

$$= \sum_{p_0=0}^{K_1N_1-1} \sum_{p_1=0}^{K_2N_2-1} \cdots \sum_{p_n=0}^{K_nN_n-1} c^{(i)}_{p_1,p_2,\ldots,p_n} W_{K_1N_1}^{-p_1P_1} W_{K_2N_2}^{-p_2P_2} \cdots W_{K_nN_n}^{-p_nP_n}, \quad (4.11)$$

where $i = 0, \ldots, (K_1K_2 \cdots K_n - 1)$. Then we assign $F^{(i)}(\vec{P})$ by the following rule

$$F^{(i)}(\vec{P}) = \begin{cases} K_1K_2 \cdots K_nF(p_1, p_2, \ldots, p_n) & ; \ \vec{P} = f(\vec{p}, i) \\ 0 & ; \ \text{otherwise} \end{cases}, \quad (4.12)$$

where $f(\vec{p}, i)$ defines the non-zero positions in transform domain for the ith new generated array. (similar to Fig. 4.1(b) in 2D case.) For a certain i, the non-zero positions in transform domain are equally spaced along all axes.

The n-dimensional IDFT is defined by $C^{(i)}(p_1, \ldots, p_n)$

$$= \frac{1}{K_1N_1K_2N_2 \cdots K_nN_n} \sum_{P_1=0}^{K_1N_1-1} \sum_{P_2=0}^{K_2N_2-1} \cdots \sum_{P_n=0}^{K_nN_n-1} F^{(i)}(\vec{P}) W_{K_1N_1}^{p_1P_1} W_{K_2N_2}^{p_2P_2} \cdots W_{K_nN_n}^{p_nP_n}. \quad (4.13)$$

By applying n-dimensional IDFT on $F^{(i)}(\vec{P})$, we obtain an array sequence $C^{(i)}$ of dimension $K_1N_1 \times K_2N_2 \times \ldots \times K_nN_n$. The CC function between any two generated array sequences is exactly zero.

Chapter 5

Preamble Structure for MIMO-OFDM WLAN Systems

5.1 Backgrounds

5.1.1 MIMO-OFDM WLAN systems

In [10], a TDMA-like preamble structure was suggested for MIMO-OFDM system. In this structure, conventional algorithms for synchronization, channel estimation, etc. in SISO-OFDM system can be extended directly since the receiver can distinguish the signals from different transmit antennas separately. However, the total length of the proposed preamble grows linearly with the number of the transmit antennas. It is not highly efficient because of the increased overhead. Moreover, when one transmit antenna is idling, the receiver cannot get any information about the idling transmitter(ex.: channel information) during this period. Hence we hope to find a more efficient preamble structure.

5.2 Proposed preamble structure

The preamble structure proposed here is based on the training symbol structure in IEEE 802.11a standard[13], which is showed in Fig. 5.1. We will focus on the long training symbol design. Channel estimation and fine frequency offset estimation are the main tasks during the long training symbols. In conventional OFDM systems, several

algorithms based on long preamble symbols are presented to work jointly to attain synchronization tasks and channel estimation. We are going to apply the new sequences that we had been discussed to be the training sequences in the MIMO-OFDM WLAN systems.

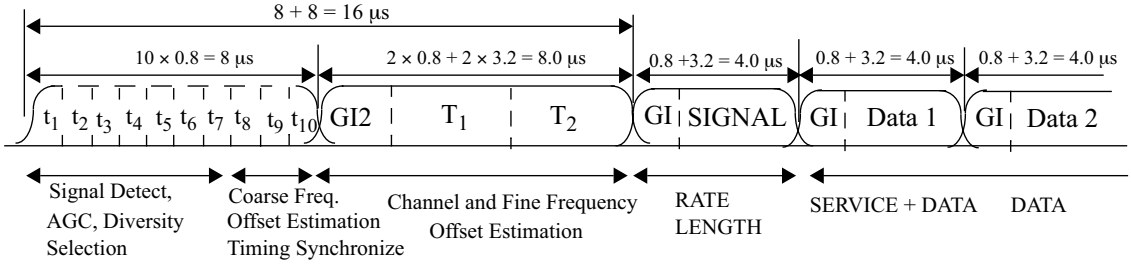

Figure 5.1: OFDM training structure in IEEE 802.11a standard. (We will redesign the long training sequences.)

In the IEEE 802.11a standard, the guard interval is of length L, and it needs to be larger than the maximum delay spread. Hence we should generate the PS sequences or our new sequences according to the length of the guard interval. Since the maximum delay spread is bounded, we can choose a suitable sequence length such that the unwanted peak values of the AC function can be avoided. By Choosing the new proposed sequences of length $N = KN_c = 16K$, where K is related to the number of transmit antennas we use, the unwanted peak values of the AC function can be avoided. Considering the system with 2 transmit antennas, we need at least two new proposed sequences with perfect CC properties. In this case, $K = 2$ and hence the period of the sequences need to be $N = 32$. To suit the long training symbol length in 802.11a standard, we simply set $K = 4$. This means this set of sequences can at most support 4 transmit antennas. Fig. 5.2 shows the structure adopted in [10]. Fig. 5.3 shows the structure we adopt. The overhead is highly reduced.

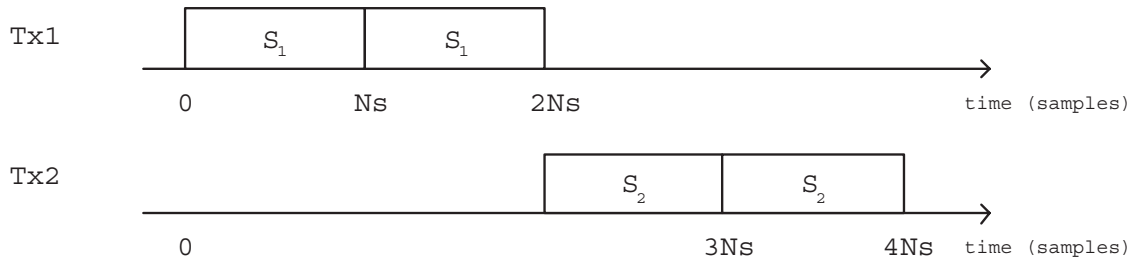

Figure 5.2: A time orthogonal preamble for a MIMO configuration with 2 transmit antennas. (The guard intervals are not shown in this figure.)

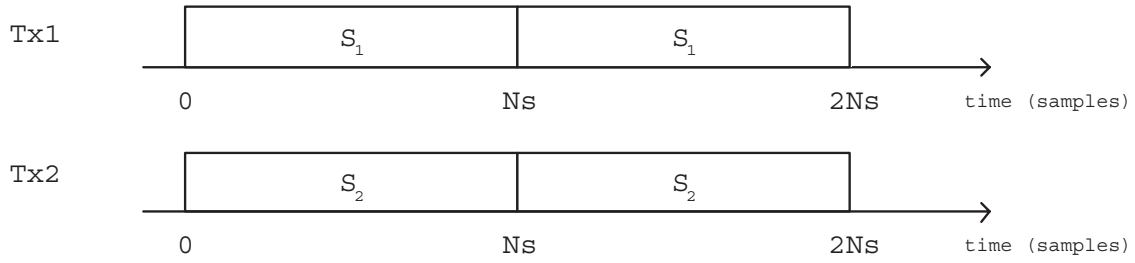

Figure 5.3: A coded orthogonal preamble for a MIMO configuration with 2 transmit antennas.

5.2.1 Cyclic prefix

The cyclic prefix parts in conventional OFDM system are still necessary for some consideration. For time-domain channel estimation algorithms, which will be introduced in chapter 6, the added cyclic prefix can help us to preserve the periodic AC and CC properties of the adopted sequences, even though we remove the cyclic prefix at the channel estimation stage. Fig. 5.4 is the suggested preamble structure for a MIMO configuration with 2 transmit antennas.

5.2.2 Length of the training sequence

We had introduced the PS sequences and a new set of orthogonal sequences in chapter 2. Both of them have periodic AC and excellent CC properties. However, our new sequences are more flexible to the sequences length. In different systems, the defined training symbol length may be not the same. For example, the length of the training

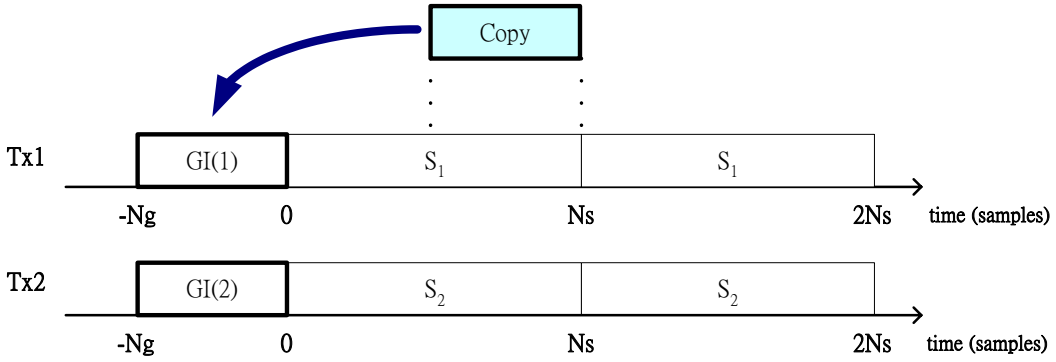

Figure 5.4: Suggested long training symbol structure for a MIMO configuration with 2 transmit antennas.

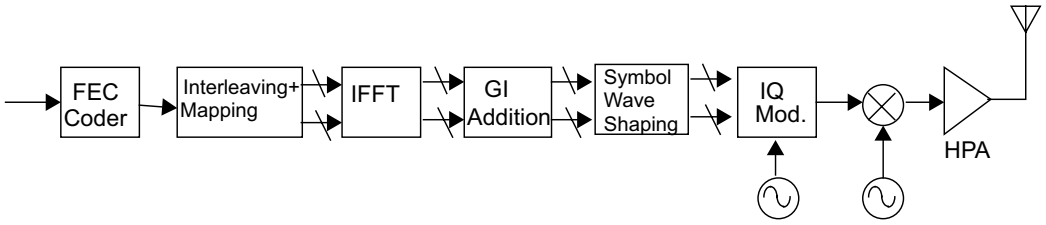

Figure 5.5: Transmitter block diagram for the OFDM PHY.

symbol defined in 802.11a and 802.16 are different. Hence a set of sequences with less constraint on the sequences length is important for preamble signal design.

5.2.3 Constraints on the constellation of training symbols

In OFDM systems [13], the OFDM subcarriers shall be modulated by using BPSK, QPSK, 16-QAM, or 64-QAM modulation depending on the transmission rate requested. The encoded and interleaved are divided into groups to form symbols and then converted into complex numbers representing BPSK, QPSK, 16-QAM, or 64-QAM constellation points. The modulation symbols are mapped to the inputs of the IDFT block. These operations are showed in Fig. 5.5. In previous discussion, we generate the training symbols in time domain. If we want to generate them from frequency domain, which is the case in IEEE 802.11a, we need to put the DFT values of these training sequences as

the input of IDFT block. The DFT values of the sequences we adopted usually do not fall on the constellations selected. Hence we propose another way to generate desired training sequence from frequency domain.

Similar to the steps introduced in section 2.2.3, we need a basis sequence of length N_c, $x(n)$, with perfect AC function first. We hope that this sequence can be generated from its IDFT, $X[k]$, and $X[k]$'s are BPSK or QPSK constellation points. By using the concepts discussed in chapter 3, we know that if all frequency components of a sequence have the same magnitude, then perfect AC property can be achieved. Hence we simply set $X(k) = \sqrt{N_c}e^{j\phi_k}$. There is no constraint on the phase of each frequency component. Therefore, we can limit the choice of $\{\phi_k\}$ to finite M-ary constellation points, i.e.,

$$\phi_k = \exp\left(j\frac{2\pi n_k}{M}\right),\ n_k \in \text{integer}. \tag{5.1}$$

Moreover, if the peak-to-average power ratio(PAPR) problem is further considered, the complementary sequences can be applied[14].

5.3 Simulation environment

Subsequent discussion addresses the issues of synchronization, channel estimation based on the proposed preamble structure. Our proposed algorithms are to be tested through computer simulation of transmission over real-world wireless channels. Table 6.1 lists some parameters adopted in the IEEE 802.11a standard. Exponentially decayed Rayleigh fading channels are used in our simulation with the impulse response given by

$$h_t = \alpha_t + j\beta_t, \tag{5.2}$$

where

$$\alpha_t = N\left(0, \frac{1}{2}\sigma_t^2\right), \tag{5.3}$$

$$\beta_t = N\left(0, \frac{1}{2}\sigma_t^2\right),\ t = 0, 1, 2, \cdots \tag{5.4}$$

$$\sigma_t^2 = \sigma_0^2 e^{-\frac{tT_s}{T_{max}}},\ \sigma_0^2 = 1 - e^{-\frac{T_s}{T_{max}}}. \tag{5.5}$$

$T_s$is the sampling period, T_{RMS} is the root mean squared delay, and T_{max} is the maximum delay spread.

There are lots of works in literatures that discuss the channel capacity of the MIMO systems, and we know that the channel capacity can be maximized if the sub-channels from different transmit antennas to every receive antenna are independent. Hence we generate the channel responses independently in our simulation.

Chapter 6

Fine Frequency Offset Estimation and Channel Estimation

6.1 Timing and frequency synchronization for SISO OFDM systems

Commonly, a repetition preamble is proposed to allow timing and frequency synchronization in digital communication systems. For SISO(Single Input and Single Output) OFDM systems, most frequency and timing estimation methods utilize the periodic nature of the time-domain signal by using a cyclic prefix, or by designing the training symbol having repeated parts. The idea of them are based on maximizing the similarity probability of the received sample sequences. In IEEE 802.11a standard, the preamble consists of ten short OFDM training symbols used for timing and carrier recovery and two identical long OFDM training symbols used for channel estimation. Schmidl and Cox [11] use a training symbol containing two identical halves to estimate the frame timing and frequency offset. We briefly describe the estimation method of [11] in section 6.1.1. Some other algorithms are also suggested with different metrics [12], but the principles are basically the same.

6.1.1 Schmidl and Cox's algorithms

Consider a OFDM system using N sub-carriers, and the sub-carrier spacing is $1/T$, where T is the OFDM symbol duration. Then the baseband signal is given by

$$u(t) = \sum_{n=0}^{N-1} c_n e^{(j2\pi f_n t)}, \quad 0 \le t \le T, \tag{6.1}$$

where $f_n = n/T$. The baseband signal is then up-converted to the radio frequency (RF) and transmitted through the channel. At the receiver end, the signal is down-converted to an intermediate frequency (IF), and demodulated. A carrier frequency offset of Δf causes a phase rotation of $2\pi t \Delta f$. We need to compensate this with some methods, otherwise it causes both a rotation of the constellation and a spread of the constellation points similar to additive white Gaussian noise (AWGN). The samples of the transmitted baseband OFDM signal $u(t)$, assuming ideal Nyquist pulse shaping, can be expressed as (excluding the cyclic prefix)

$$u(k) = \sum_{n=0}^{N-1} c_n e^{(j2\pi kn/N)}, \quad 0 \le k \le N-1, \tag{6.2}$$

with the sampling period is T/N. At the receiver, the samples are

$$r(k) = e^{j2\pi vk/N} u(k) + n(k), \tag{6.3}$$

where is the carrier frequency offset normalized to subcarrier spacing; i.e., $v \cdot 1/T = \Delta f$.

Assume that our training symbol have two identical halves(excluding the cyclic prefix), and each of them is of length $L = N/2$. Let the sum of the pairs of products be

$$P(d) = \sum_{m=0}^{L-1} (r^*_{d+m} r_{d+m+L}), \tag{6.4}$$

where d a time index corresponding to the first sample in a window of $2L$ samples. This window slides along in time as the receiver searches for the first training symbol. The received energy for the second half-symbol is defined by

$$R(d) = \sum_{m=0}^{L-1} |r_{d+m+L}|^2. \tag{6.5}$$

The timing metric can be defined as

$$M(d) = \frac{|P(d)|^2}{(R(d))^2}. \tag{6.6}$$

The estimated frame timing

$$\hat{d} = \max_d M(d) \tag{6.7}$$

The main difference between the two halves of the training symbol will be a phase difference of

$$\phi = \pi T \Delta f \tag{6.8}$$

which can be estimated by

$$\hat{\phi} = \text{angle}(P(\hat{d})). \tag{6.9}$$

Fig. 6.1 gives a typical metric plot when Schmidl and Cox's synchronization algorithm is adopted.

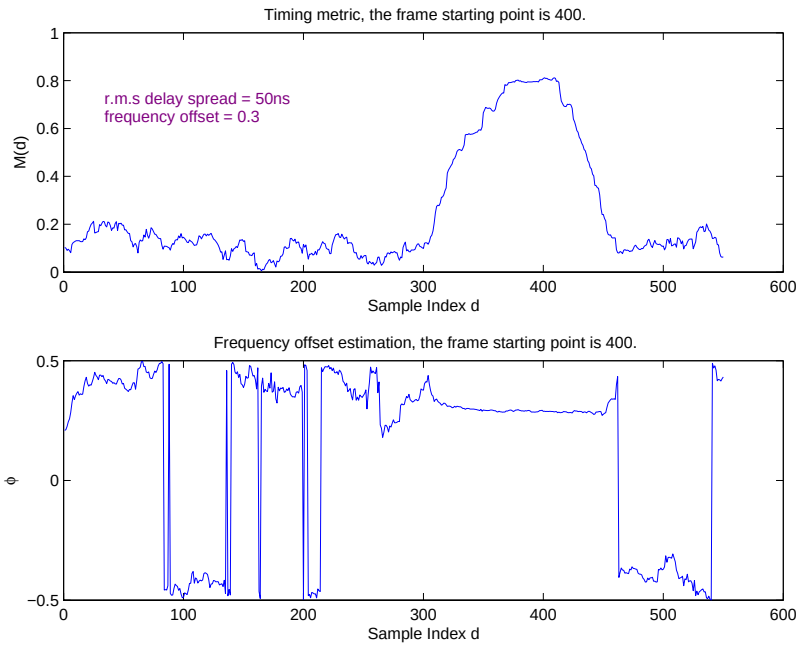

Figure 6.1: A typical result of Schmidl and Cox's synchronization algorithm. The estimated frequency offset is in unit of the subcarrier spacing. (Parameters: r.m.s. delay spread = 50ns, frequency offset = 0.3 subcarrier spacing, and SNR = 10dB.)

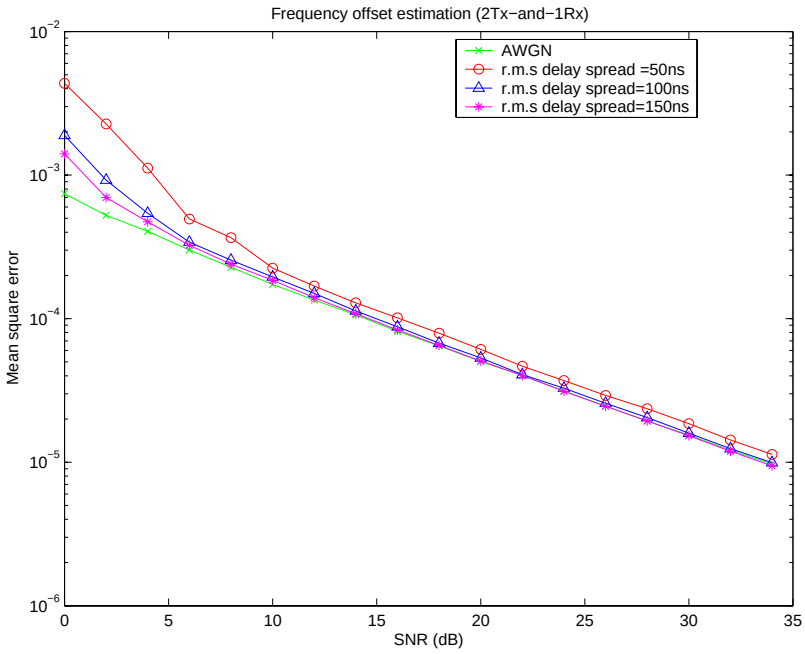

Figure 6.2: MSE of the frequency offset estimator in different multi-path environments (2Txs and 1 Rx). Frequency offset = 0.3 subcarrier spacing.

6.2 Frequency synchronization schemes for MIMO-OFDM systems

We apply the synchronization algorithm for conventional OFDM systems to MIMO systems directly. Here we make some assumptions that the first rays of the signals emitted from all the transmit antennas arrive at the receive antennas at the same time, and the frequency offsets corresponding to all different paths are the same. For the case that multiple transmit antennas and single receive antenna are used, the metric computation formula is still the same as (6.6), but the received signal model becomes

$$r(k) = \sum_{i=1}^{N_t} e^{j2\pi vk/N} u_i(k) + n(k). \tag{6.10}$$

For the case that multiple receive antennas are also used, we can apply some diversity combining schemes to provide better performance. Fig. 6.2 shows the simulation result for channels with different delay spread. We can observe that the frequency offset

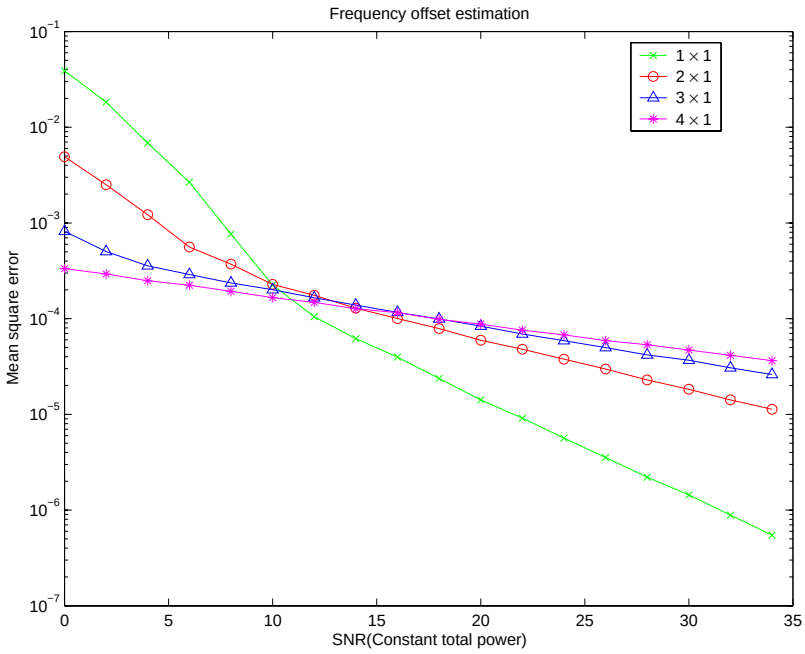

Figure 6.3: MSE of the frequency offset estimator for systems of different number of transmit antennas. (Frequency offset=0.3 subcarrier spacing and r.m.s. delay spread=50ns.)

estimator has better performance when operated in a environment with larger delay spread. Fig. 6.3 shows the performance for systems with different number of transmit antennas under the same environment. The total transmit power is constant.

6.3 Channel Estimation

6.3.1 System model

With the proposed preamble structure, the receiver end can separate the signals originated from different transmit antennas. Hence we can estimate the channel impulse responses of all different sub-channels with the aid of the knowledge of the preamble signals. Here we take the simplest system, a 2×1 systems (2 transmit antennas and one receive antenna, see Fig. 6.4), as an example without loss of generality. Fig. 5.4 shows the corresponding preamble structure. Notice that the cyclic prefix (or guard interval) is necessary to maintain the good periodic AC and CC properties. The receive antenna

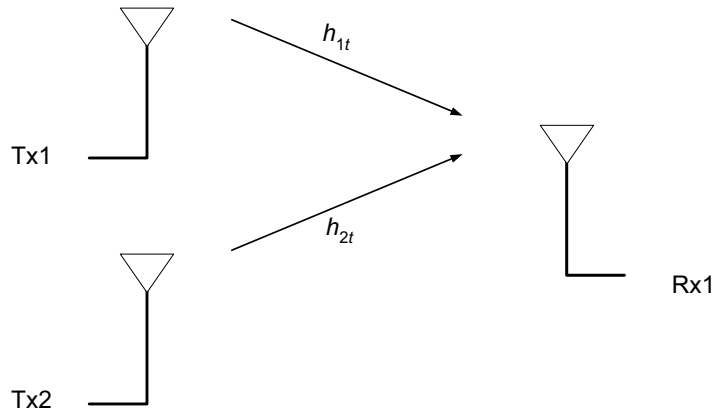

Figure 6.4: A system with two transmit antennas and one receive antenna.

need two matched filters to estimate channel responses. We describe the algorithm as follows.

System model:

The transmitted data vector from k'th transmit antenna during the preamble is written as

$$[s_{k0}, s_{k1}, \ldots, s_{k(N_s-1)}, s_{kN_s}, s_{k(N_s+1)}, \ldots, s_{k(2N_s-1)}]^T, \quad k = 1, 2. \tag{6.11}$$

Notice that the s_{kt}'s are the preamble signals and $s_{kt} = s_{k(t+N_s)}$ for $t = 1, \ldots, N_s$.

With correct frame timing synchronization and perfect frequency offset compensation, the processed received samples during the preamble can be expressed as: (cyclic prefix is removed)

$$\vec{r} \;=\; [r_0, r_1, \ldots, r_{N_s-1}, r_{N_s}, r_{N_s+1}, \ldots, r_{2N_s-1}]^T. \tag{6.12}$$

The element r_i in the received vector can be written as

$$r_i = \sum_{t=0}^{L-1} [h_{1t} s_{1(i-t)} + h_{2t} s_{2(i-t)}] + n_i, \tag{6.13}$$

where $\{h_{1t}\}$ and $\{h_{2t}\}$ are the channel impulse responses corresponding to the two different sub-channels, and the n_i's are modelled as additive white Gaussian noise. The

length of channel response is assumed to be less than or equal to L. Our goal is to extract the information of $\{h_{1t}\}$ and $\{h_{2t}\}$ from the received data vector.

6.3.2 A least square error channel estimator

Define $\vec{r}(t) = [r_t, r_{t+1}, \ldots, r_{t+N_s-1}]^T$ and $\vec{s}_k = [s_{k0}, s_{k1}, \ldots, s_{k(N_s-1)}]^T$. For correct frame timing, i.e., $t = 0$, and correct frequency offset compensation, ignoring the time index, the receive signal can be expressed as:

$$\vec{r} = \mathbf{S}\mathbf{h} + \vec{n} = [\mathbf{S}_1\mathbf{S}_2] \begin{bmatrix} \vec{h}_1 \\ \vec{h}_2 \end{bmatrix} + \vec{n}, \tag{6.14}$$

where

$$\mathbf{S}_i = \begin{bmatrix} s_{i0} & s_{i(-1)} & \cdots & s_{i(-L+1)} \\ s_{i1} & s_{i0} & \cdots & s_{i(-L+2)} \\ \vdots & \vdots & & \vdots \\ s_{i(N_s-1)} & s_{i(N_s-2)} & \cdots & s_{i(-L+N_s)} \end{bmatrix}_{N_s \times L} \tag{6.15}$$

Notice that $s_{i(-t)} = s_{i(N_s-t)}$ for $1 \leq t < L$ since cyclic prefix is added. The least square channel estimator becomes

$$\hat{\mathbf{h}} = \begin{bmatrix} \hat{\vec{h}}_1 \\ \hat{\vec{h}}_2 \end{bmatrix} = (\mathbf{S}^H\mathbf{S})^{-1}\mathbf{S}^H\vec{r}, \tag{6.16}$$

if the matrix $\mathbf{S}^H\mathbf{S}$ is full rank. For zero-mean white Gaussian noise, the channel estimation mean squared error is

$$\begin{aligned} \text{MSE} &= E[(\mathbf{h} - \hat{\mathbf{h}})^H(\mathbf{h} - \hat{\mathbf{h}})] \\ &= \sigma_n^2 \text{trace}\{(\mathbf{S}^H\mathbf{S})^{-1}\} \\ &= \sigma_n^2 \sum_i \frac{1}{\lambda_i}, \end{aligned} \tag{6.17}$$

where λ_i's are the eigenvalues of the matrix $(\mathbf{S}^H\mathbf{S})$. Now we want to minimize the term $\sum_i \frac{1}{\lambda_i}$. But we have some constraint on the eigenvalues λ_i's. The total energy of the training sequences need to be a constant, i.e., trace$\{\mathbf{S}\mathbf{S}^H\}$ should be a constant. Also, we have the equality that trace$\{\mathbf{S}\mathbf{S}^H\} = \sum_i \lambda_i$. So the problem is reduced to:

$$\begin{cases} \text{minimize} & \sum_i \frac{1}{\lambda_i} \\ \text{subject to} & \sum_i \lambda_i = \text{constant}. \end{cases}$$

This can be solved by the method of Lagrange's multipliers[15]. The optimum solution must satisfy $\mathbf{S}^H\mathbf{S} = E_s\mathbf{I}$, where E_s is a constant. We can verify that our training sequences satisfy this criterion with $E_s = N_s$ since the training sequences we adopted have good AC properties within the maximum lags L and perfect CC properties between different sequences. Hence the estimator can be further reduced to

$$\hat{\mathbf{h}} = \begin{bmatrix} \hat{\vec{h}}_1 \\ \hat{\vec{h}}_2 \end{bmatrix} = \frac{1}{N_s}\mathbf{S}^H\vec{r}. \tag{6.18}$$

The implementation of the estimator for one sub-channel is simply a matched filter.

Since the contents of the two training symbols are identical, and the noise samples are statistically independent, averaging them can be used to improve the quality of the channel estimate. This is a common way to lower the noise variance in OFDM systems because of the repeated preamble structure. Hence the modified channel estimator becomes:

$$\hat{\mathbf{h}} = \begin{bmatrix} \hat{\vec{h}}_1 \\ \hat{\vec{h}}_2 \end{bmatrix} = \frac{1}{2N_s}\mathbf{S}^H[\vec{r}(0) + \vec{r}(N_s)]. \tag{6.19}$$

The results we have can be extended to the system with multiple transmit antennas.

6.3.3 Numerical results

Reported in this subsection is some numerical simulation results for our channel estimation algorithm. Table 6.1 lists some simulation parameters. Fig. 6.5 shows the estimation result for one sub-channel for the case that the r.m.s. delay spread is 50ns. The lower bound of the performance is also depicted in this figure. We can provide better performance by averaging because of the repeated preamble structure. For the cases that the channel response length is within the guard interval length, the optimal performance can be obtained, and it is independent of the channel response length. For the case that the channel response length is slightly longer than guard interval, the performance does not degrade seriously. Generally speaking, the channel gains with delay larger than guard interval length are small enough such that we can just ignore them.

Fig. 6.6 shows the simulation result for channels with different r.m.s. delay spread.

In this chapter, the channel estimation is done in time domain. Of course, we still can estimate the channel responses in frequency domain since the training symbols occupy different bands for different transmit antennas. However, the performance will degrade. Generally speaking, the time-domain channel estimator outperforms the frequency-domain channel estimator when the mean squared channel estimation error is considered [16][17]. In our case, if we want to estimate the channel response in frequency domain, the performance will degrade more than the cases in SISO systems. This is because that we need some interpolation algorithms to estimate the frequency channel responses which are with no training tones. The "interpolation" will induce more estimation error.

Sample period	50ns	Sequence parameters	
Guard interval	16 (samples)	K	4
Training symbol length	64 (samples)	$N_c(N_b{}^2)$ (AC period)	16

Table 6.1: Some simulation parameters adopted.

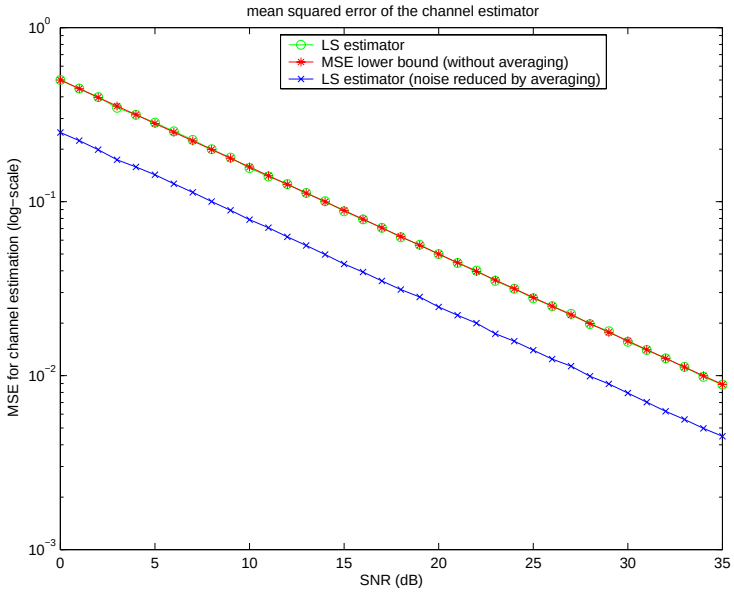

Figure 6.5: Mean squared channel estimation error. Noise variance can be reduced by averaging.

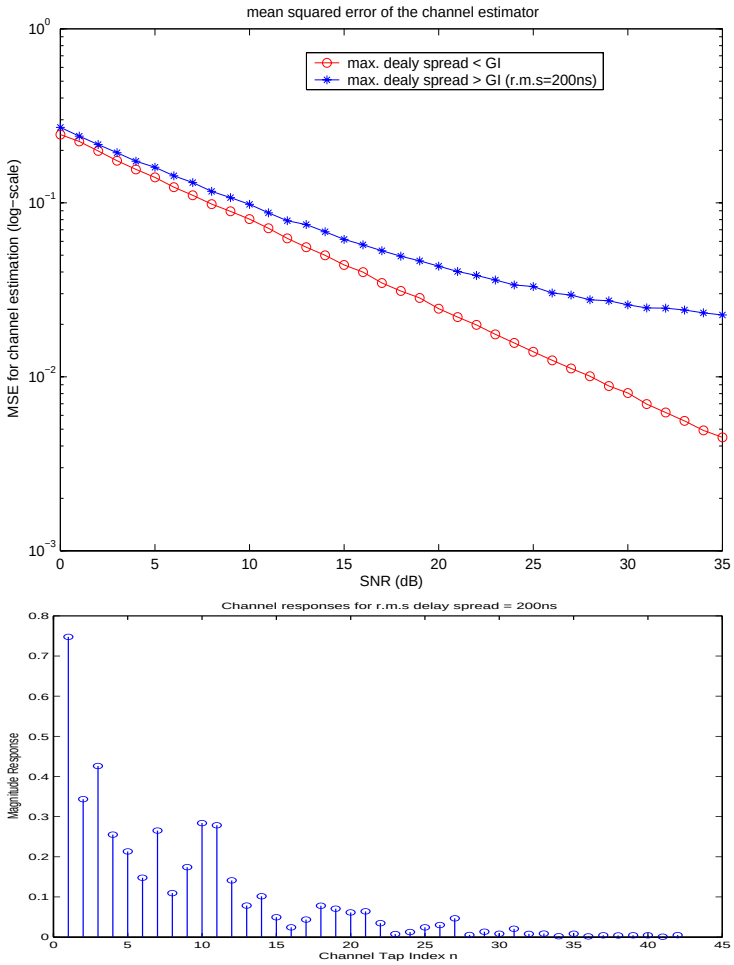

Figure 6.6: Mean squared channel estimation error for different channel delay spread.(Guard Interval = 16 samples.)

Chapter 7

Conclusion

A set of training sequences for a multiple antenna system should have perfect AC and CC properties within the maximum delay spread. This thesis presents a systematic transform domain approach for generating such sequences. Preambles based on these new sequences can be used in MIMO-OFDM WLAN systems. The new preamble sequences can be regarded as a generalization of the PS sequences proposed in [3] for both can be generated by the same approach with different constraints. We show that the AC function and CC function are closely related to the DFTs of the desired sequences. Our method renders a natural interpretation and rigorous proof of the perfect AC function of the sequences proposed in [8].

The relationships between some parameters of the sequences and the system specifications are established. Once the length of the OFDM guard interval is given, the length of training sequence is determined by the number of the transmit antennas. We provide a good solution when the elements of training sequence are limited to a finite constellation. We also propose synchronization and channel estimation algorithms based on the suggested preamble structure. Numerical simulation indicates that, since our preamble sequences possess the desired properties, our channel estimator yields optimal performance.

Several theoretical and implementation issues remain to be settled. For example, the effects of I-Q imbalance, nonlinear distortions, Doppler offset and Doppler spread are

likely to destroy and distort the original AC or CC properties, the robustness against these channel or signal jitters is of great concern to both practitioners and theorists. On the other hand, there are reports about the application of multi-dimensional signature sequences for MIMO-OFDMA or other MIMO MA systems. Multi-dimensional signature sequences for Radar and sonar applications, though require different AC and/or CC properties, have been studied before as well. But the design of these sequences usually does not adopt the transform domain approach but involves a variety of other combinatorial and ad hoc techniques. We believe that our approach can provide a avenue for discovering new sequences with desired properties.

Bibliography

[1] R. L. Peterson, R. E. Ziemer, and D.E. Borth, *Introduction to spread spectrum communications*, Prentice Hall, 1995.

[2] R. A. Scholtz, and L. R. Welch, "Group characters: sequences with good correlation properties", *IEEE Trans. Inform. Theory*, vol. IT-24, pp. 537-545, Sep. 1978.

[3] S. I. Park, S. R. Park, I. Song, and N. Suehiro, "Multiple-access interference reduction for QS-CDMA systems with a novel class of polyphase sequences", *IEEE Trans. Inform. Theory*, vol. 46, pp. 1448-1458, July 2000.

[4] L. R. Welch, "Lower bounds on the maximum cross correlation of signals", *IEEE Trans. Inform. Theory*, vol. IT-20, pp. 396-399, May 1976.

[5] D. V. Sarwate, "Bounds on cross correlation and autocorrelation of sequences", *IEEE Trans. Inform. Theory*, vol. IT-25, pp. 720-724, Nov. 1979.

[6] R. L. Frank and S. Zadoff, "Phase shift codes with good periodic correlation properties," *IEEE Trans. Inform. Theory*, vol. IT-8, pp. 381-382, Oct. 1962.

[7] D. C. Chu, "Polyphase codes with good periodic correlation properties," *IEEE Trans. Inform. Theory*, vol. IT-18, pp. 531-532, July 1972.

[8] N. Suehiro and M. Hatori, "Modulatable orthogonal sequences and their application to SSMA systems," *IEEE Trans. Inform. Theory*, vol. 34, pp. 93-100, Jan. 1988.

[9] P. Z. Fan and M. Darnell, *Sequence design for communications applications*, London, U.K.: Research Studies Press Ltd, 1996.

[10] A. van Zelst, T.C.W. Schenk, "Implementation of a MIMO OFDM-based wireless LAN system," *IEEE Trans. Signal Processing*, vol. 52, no.2, pp. 82-88, Feb. 2004.

[11] T. M. Schmidl and D. C. Cox, "Robust frequency and timing synchronization for OFDM," *IEEE Trans. Commun.*, vol. 45, pp. 1613-1621, Dec 1997.

[12] J.-J. van de Beek, M. Sandell, and P. O. Borjesson, "ML estimation of time and frequency offset in OFDM systems," *IEEE Trans. Signal Processing*, vol. 45, pp. 1800-1805, July 1997.

[13] *Wireless LAN Medium Access Control* (MAC) and Physical Layer (PHY) Specifications, In IEEE Std 802.11-1999, 1999.

[14] B. M.Popovic, "Synthesis of power efficient multitone signals with flat amplitude spectrum," *IEEE Trans. Commun.*, vol. 39, pp. 1031-1033, July 1991.

[15] G. Caire and U. Mitra, "Training sequence design for adaptive equalization of multi-user systems," in *Proc. 32nd Asilomar Conf.*, vol. 2, pp. 1479-1483, 1998.

[16] W. Chen and U. Mitra, "Training sequence optimization: Comparisons and an alternative criterion," *IEEE Trans. Commun.*, vol. 48, pp. 1987-1991, Dec. 2000.

[17] Z. Cheng and D. Dahlhaus, "Time versus Frequency Domain Channel Estimation for OFDM Systems with Antenna Arrays," *Proc. of the 6th International Conference on Signal Processing (ICSP'02)*, vol. 2, pp. 1340-1343, Aug. 26-30, 2002.

作　者　簡　歷

蔡隆盛，台南市人，1980 年生。

1996 ~ 1998：省立台南二中。

1998 ~ 2002：國立清華大學電機工程學系。

2002 ~ 2004：國立交通大學電信工程學系碩士班。

Graduate Course

1. Spread Spectrum Communications
2. Information Theory
3. Digital Communications
4. Random Process
5. Digital Signal Processing
6. Detection and Estimation
7. Array Signal Processing
8. Coding Theory
9. Design of Communication System VLSI Chips and Circuits
10. Digital Receivers
11. Analog Circuit Design
12. Digital Integrated Circuit Design and Modeling
13. Semiconductor Microwave Device